The C terminus of p53 regulates gene expression by multiple mechanisms in a target- and tissue-specific manner in vivo

Pierre-Jacques Hamard,[1] Nicolas Barthelery,[1,2,4] Brandon Hogstad,[1,2,4] Sathish Kumar Mungamuri,[1] Crystal A. Tonnessen,[1,2] Luis A. Carvajal,[1,2] Emir Senturk,[1,2] Virginia Gillespie,[3] Stuart A. Aaronson,[1,2] Miriam Merad,[1,2] and James J. Manfredi[1,2,5]

[1]Department of Oncological Sciences, [2]The Graduate School of Biomedical Sciences, [3]Center for Comparative Medicine and Surgery, Mount Sinai School of Medicine, New York, New York 10029, USA

The p53 tumor suppressor is a transcription factor that mediates varied cellular responses. The C terminus of p53 is subjected to multiple and diverse post-translational modifications. An attractive hypothesis is that differing sets of combinatorial modifications therein determine distinct cellular outcomes. To address this in vivo, a *Trp53*$^{\Delta CTD/\Delta CTD}$ mouse was generated in which the endogenous p53 is targeted and replaced with a truncated mutant lacking the C-terminal 24 amino acids. These *Trp53*$^{\Delta CTD/\Delta CTD}$ mice die within 2 wk post-partum with hematopoietic failure and impaired cerebellar development. Intriguingly, the C terminus acts via three distinct mechanisms to control p53-dependent gene expression depending on the tissue. First, in the bone marrow and thymus, the C terminus dampens p53 activity. Increased senescence in the *Trp53*$^{\Delta CTD/\Delta CTD}$ bone marrow is accompanied by up-regulation of *Cdkn1* (p21). In the thymus, the C-terminal domain negatively regulates p53-dependent gene expression by inhibiting promoter occupancy. Here, the hyperactive p53$^{\Delta CTD}$ induces apoptosis via enhanced expression of the proapoptotic *Bbc3* (Puma) and *Pmaip1* (Noxa). In the liver, a second mechanism prevails, since p53$^{\Delta CTD}$ has wild-type DNA binding but impaired gene expression. Thus, the C terminus of p53 is needed in liver cells at a step subsequent to DNA binding. Finally, in the spleen, the C terminus controls p53 protein levels, with the overexpressed p53$^{\Delta CTD}$ showing hyperactivity for gene expression. Thus, the C terminus of p53 regulates gene expression via multiple mechanisms depending on the tissue and target, and this leads to specific phenotypic effects in vivo.

[*Keywords*: p53; gene expression; tissue specificity; C terminus; hematopoiesis; mouse]

Supplemental material is available for this article.

Received June 14, 2013; revised version accepted July 29, 2013.

The p53 tumor suppressor is a transcription factor that mediates a variety of cellular responses. The best characterized of these include cell cycle arrest, which, if sustained, leads to senescence and apoptosis (Vousden and Prives 2009). The p53 protein is kept inactive through interactions with several negative regulators, most notably Mdm2 (Luo et al. 2004; Kruse and Gu 2009; Vousden and Prives 2009; Manfredi 2010). It has been proposed that post-translational modifications of p53 are critical to disrupt its binding to Mdm2 and facilitate its interaction with cofactors, resulting in a p53 protein that is robust in its ability to transcriptionally regulate target gene expression (Kruse and Gu 2009; Manfredi 2010). The C terminus of p53 in particular is subjected to multiple and diverse post-translational modifications (Kruse and Gu 2009; Carvajal and Manfredi 2013) quite similar to that seen with histone tails (Kouzarides 2007). An attractive hypothesis is that differing sets of combinatorial modifications therein determine distinct cellular outcomes (Carvajal and Manfredi 2013).

The C terminus was originally characterized as playing a key role in sequence-specific DNA binding by p53 (Hupp et al. 1992). Its excess of basic residues contributes to its ability to bind to DNA, albeit nonspecifically. It had been proposed that this region of p53 interferes with the ability of the core domain to bind response elements with sequence specificity and therefore has a negative regulatory function (Anderson et al. 1997; Ahn and Prives 2001). This notion was discredited by studies suggesting that this may be an artifact of the particular in vitro DNA-binding assays being used (Espinosa and Emerson 2001), although this remains controversial (Luo et al. 2004; Kruse and Gu 2009; Vousden and Prives 2009; Carvajal and

[4]These authors contributed equally to this work.
[5]Corresponding author
E-mail james.manfredi@mssm.edu
Article is online at http://www.genesdev.org/cgi/doi/10.1101/gad.224386.113.

Manfredi 2013). Experiments in cell culture were more in line with a positive role for the C terminus (Chen et al. 1996; Kruse and Gu 2009; Hamard et al. 2012; Carvajal and Manfredi 2013). These supported a role in tracking of p53 on genomic DNA (McKinney et al. 2004; Kruse and Gu 2009; Carvajal and Manfredi 2013) as well as serving as recruitment sites for transcriptional cofactors (Barlev et al. 2001; Mujtaba et al. 2004). The challenge in interpreting such experiments is that they rely on ectopic expression of an exogenously introduced p53, often overexpressed at a nonphysiologically relevant level.

To gain more definitive insight into the role of this region of p53, a *Trp53*$^{\Delta CTD/\Delta CTD}$ mouse was generated that replaces the endogenous p53 with a truncated form of p53 that lacks the C-terminal 24 amino acids. In spite of presenting a wild-type phenotype immediately after birth, *Trp53*$^{\Delta CTD/\Delta CTD}$ mice quickly degenerate and die within 2 wk post-partum. Two main phenotypes are observed: a hematopoietic failure and an abnormal cerebellar development. The C terminus of p53 is shown to regulate gene expression at several levels: p53 accumulation, genomic site occupancy, or transcriptional activation. The precise mechanism depends on the tissue and target, thereby conferring specific phenotypic effects in vivo.

Results

Generation of the Trp53$^{\Delta CTD/\Delta CTD}$ *mouse*

To generate a *Trp53*$^{\Delta CTD/\Delta CTD}$ mouse that lacks the C-terminal 24 amino acids of p53, a knock-in strategy was used (Fig. 1A). To enable future studies with targeted expression of the deletion mutant, a *Trp53*$^{NEO/NEO}$ mouse was first generated by means of a targeting vector harboring two exon 11s separated by a *NEO* selection cassette (see the Supplemental Material for details on the construction of the targeting vector). The resulting targeted *Trp53*^{NEO} allele contains a wild-type exon 11 in frame with the rest of the upstream gene and enables the expression of a full-length (FL), wild-type p53 protein along with the shorter mouse-specific alternative spliced form, p53AS (Bienz et al. 1984). Two *loxP* recombination sites within intron 10 and downstream from the *NEO* cassette, respectively, enable the excision of the first wild-type exon 11 along with the *NEO* cassette after recombination with the *CRE* recombinase. The resulting *Trp53*$^{\Delta CTD}$ allele contains the mutated exon 11 in frame with the rest of the gene and enables the expression of a truncated p53 protein (p53$^{\Delta CTD}$) along with the shorter mouse-specific alternative spliced form (p53AS) as well. Two *FRT* recombination sites located within intron 10 and in the 3′ untranslated region (UTR) have been introduced for future studies using murine embryonic fibroblasts (MEFs) derived from *Trp53*$^{NEO/NEO}$ or *Trp53*$^{\Delta CTD/\Delta CTD}$ animals.

Trp53$^{NEO/+}$ heterozygous mice were viable and appeared phenotypically normal. They were intercrossed to generate *Trp53*$^{NEO/NEO}$ mice, which were also viable and indistinguishable from *Trp53*$^{+/+}$ animals, and were born at the expected Mendelian ratio (Supplemental Fig. 1A). To ascertain that the CRE-driven recombination was functional, MEFs were derived from embryonic day 14.5 (E14.5) embryos and treated with increasing doses of a *CRE*-expressing adenovirus (Ad-CRE) (Supplemental Fig. 1B). Using genomic DNA from MEFs of +/+, NEO/+, and NEO/NEO genotypes, recombination was observed at a multiplicity of infection (MOI) as low as 100, and the nonrecombined DNA was undetectable in *Trp53*$^{NEO/NEO}$ MEFs at MOI = 500. To confirm that the recombination occurring at the genomic DNA level was giving rise to the shorter p53$^{\Delta CTD}$ protein, MEFs were treated with Ad-CRE for 24 h and then treated with the DNA-damaging agent doxorubicin (DOX) for another 24 h at the indicated dose (Fig. 1B). Long running times were necessary to observe the difference in size between wild-type and p53$^{\Delta CTD}$ proteins. *Trp53*$^{NEO/NEO}$ mice were crossed with Protamine-*CRE* (PrmCre) mice to generate *Trp53*$^{NEO/+}$ *CRE*-expressing males. These males were intercrossed with wild-type C57BL/6J females to generate *Trp53*$^{\Delta CTD/+}$ heterozygous mice, which were born at the expected Mendelian ratio (data not shown), with no phenotypic difference from wild-type mice. Ultimately, these heterozygous mice were bred to obtain *Trp53*$^{\Delta CTD/\Delta CTD}$ homozygous animals. To confirm that these animals were expressing the truncated form of p53, MEFs derived from E14.5 *Trp53*$^{+/+}$ and *Trp53*$^{\Delta CTD/\Delta CTD}$ embryos were treated with the proteasome inhibitor MG132 to attain discernable amounts of p53 protein and analyzed by immunoblotting. Similar to what was observed in NEO/NEO MEFs, a shorter form of p53 could be seen in ΔCTD/ΔCTD MEFs (Fig. 1C). The PAb421 monoclonal antibody has an epitope that is located within the C terminus of p53. An immunoprecipitation using this antibody confirmed that the protein expressed in the ΔCTD/ΔCTD cells lacked the PAb421 epitope (Fig. 1C).

Deletion of the C-terminal 24 amino acids from p53 leads to postnatal developmental defects and death within 2 wk post-partum

Mice homozygous for deletion of the p53 C terminus displayed a striking phenotype after birth. Although the mutant pups did not show any significant phenotypic difference from their +/+ and heterozygous littermates at day 1 post-partum (P1) (Fig. 2A), these animals were markedly reduced in size and weight by P10 (Fig. 2A,B) and died within 2 wk post-partum (Fig. 2C). They exhibited several developmental defects, including kinked tails, abnormal tail tip, and digit pigmentation, and significant ataxia suggestive of underlying neurological defects. Their organs were isolated and weighed at P1 and P10. The tibia, thymus, and spleen were dramatically reduced in size, while the liver and kidney were unaffected, and the heart was enlarged (Fig. 2D; Supplemental Fig. 2A,D). The observed cardiomegaly is reminiscent of that seen in *Trp53*$^{7KR/7KR}$ mutants after irradiation (Wang et al. 2011) and is likely a compensatory consequence of the severe anemia these mutant mice present at P10. Mutant tibias were reduced in size and weight, and the red color associated with the bone marrow was not observed (Fig. 2D). Indeed, when assessed by complete blood

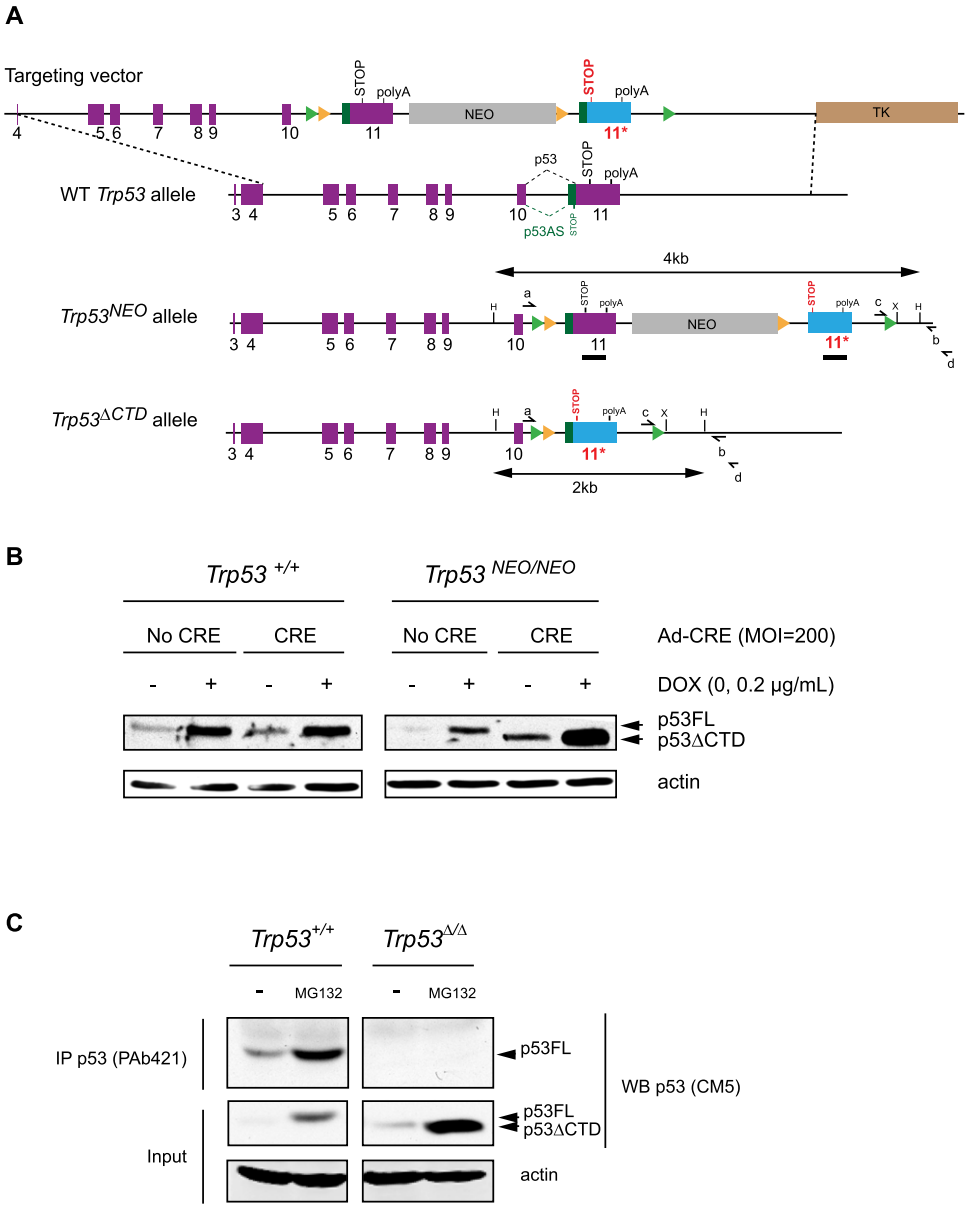

Figure 1. Generation of mice expressing a p53 protein devoid of its C-terminal domain. (*A*) Schematic of the targeting construct harboring two exon 11s separated by a *NEO* selection cassette. The resulting targeted $Trp53^{NEO}$ allele contains a wild-type exon 11 in frame with the rest of the gene and enables for the expression of a FL, wild-type p53 protein along with the shorter mouse-specific alternative spliced form (p53AS). After CRE recombination, the first wild-type exon 11 and the *NEO* cassette are excised, resulting in a $Trp53^{\Delta CTD}$ allele that contains the second exon 11, which includes a STOP mutation at position 367. The $Trp53^{\Delta CTD}$ allele encodes for a truncated p53 protein ($p53^{\Delta CTD}$) that lacks the last 24 amino acids as well as the p53AS isoform. The genotyping strategies are detailed in the Supplemental Material and Supplemental Figure 1. (Yellow triangles) loxP sites; (green triangles) FRT sites; (H) HindIII; (X) XhoI; (black bar) Southern blot probe; (a & b, c, and d) primers used for genotyping; (TK) thymidine kinase. (*B*) Immunoblot shows p53 protein expression in MEFs derived from $Trp53^{+/+}$ and $Trp53^{NEO/NEO}$ animals before or after CRE recombination. The cells were infected with an adenovirus expressing the CRE recombinase at MOI = 200 to induce the expression of the truncated form. Twenty-four hours later, cells were treated with DOX at the final concentration of 0.2 μg/mL to reach appreciable levels of p53, and 24 h after treatment, cells were harvested, and immunoblotting analysis was conducted. β-Actin was used as a loading control. p53FL and p53ΔCTD are almost indistinguishable in size, and long running times and large gels were necessary to observe the difference in migration. (*C*) Immunoprecipitation of p53 in MEFs derived from $Trp53^{+/+}$ and $Trp53^{\Delta CTD/\Delta CTD}$ animals with the p53CTD-specific monoclonal antibody PAb421. The cells were treated for 6 h with the proteasome inhibitor MG132 at a final concentration of 40 μM to reach appreciable levels of p53. The PAb421 antibody fails at precipitating the truncated p53 protein from $Trp53^{\Delta CTD/\Delta CTD}$ cells. A 5% input was immunoblotted for p53, and β-actin was used as a loading control.

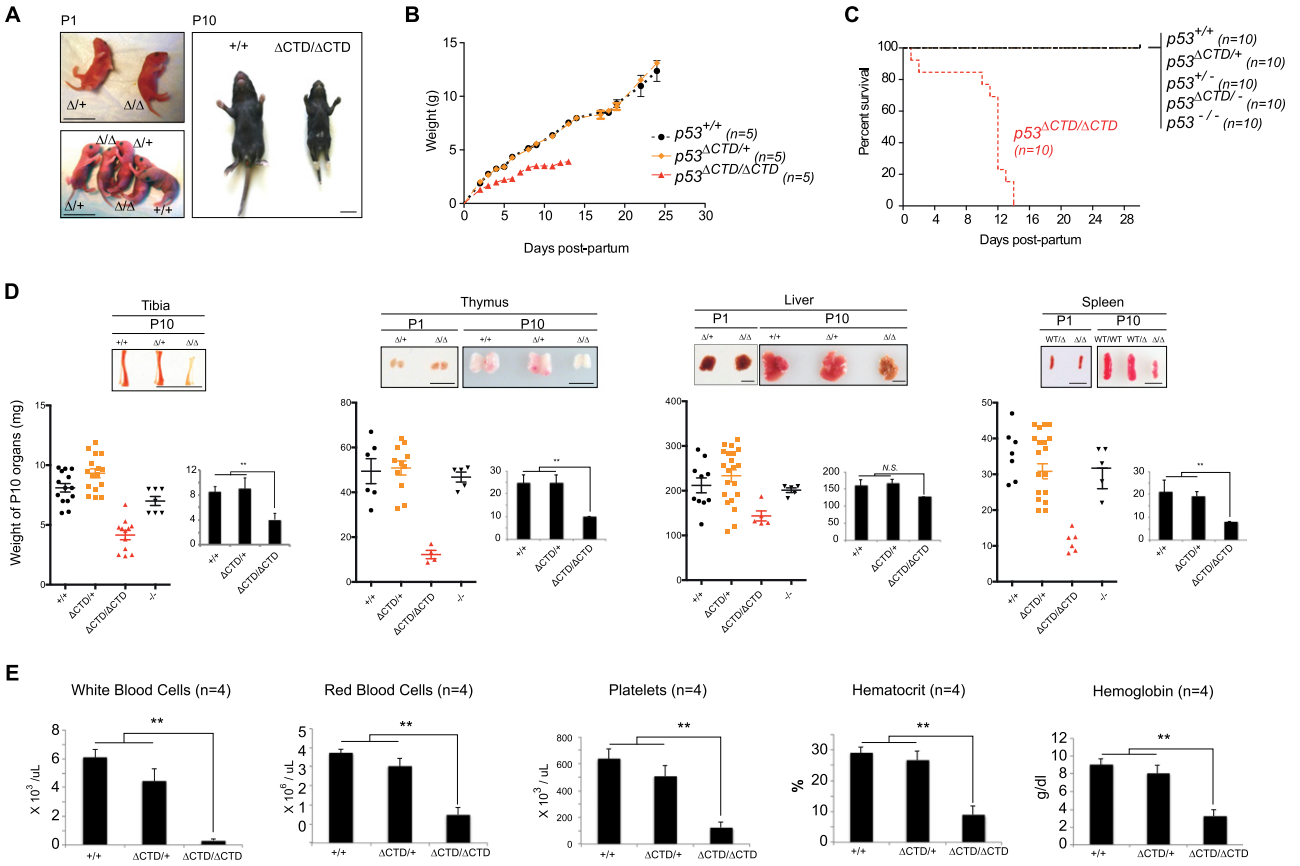

Figure 2. Deletion of the C-terminal 24 amino acids from p53 leads to postnatal developmental defects and death within 2 wk post-partum. (*A*) Pictures of whole animals at P1 show no difference between littermates of different genotypes (*Trp53*$^{+/+}$, *Trp53*$^{\Delta CTD/+}$, and *Trp53*$^{\Delta CTD/\Delta CTD}$). At P10, *Trp53*$^{\Delta CTD/\Delta CTD}$ animals are smaller than their wild-type counterparts and exhibit several developmental defects, including kinked tails, abnormal tail tip, and digit pigmentation. Bar, 1 cm. (*B*) Weight curve shows marked growth retardation for *Trp53*$^{\Delta CTD/\Delta CTD}$ animals but no significant difference between *Trp53*$^{+/+}$ and *Trp53*$^{\Delta CTD/+}$ mice. (*C*) Survival curves spanning 30 d post-partum illustrate 100% death within 2 wk for *Trp53*$^{\Delta CTD/\Delta CTD}$ animals, whereas all other genotypes survive. (*D*) Pictures of P1 and P10 whole organs demonstrate no significant difference between all genotypes at P1 but marked anemia and reduction in size for most *Trp53*$^{\Delta CTD/\Delta CTD}$ organs at P10. Weight graphs of P10 whole organs show reduced weight for *Trp53*$^{\Delta CTD/\Delta CTD}$ spleen, thymus, and tibias but not the liver and no significant difference between *Trp53*$^{+/+}$ and *Trp53*$^{\Delta CTD/+}$ organs. Bar, 0.4 cm. (*E*) Complete blood counts reveal a marked reduction of white and red blood cells, platelets, hematocrit percentage, and hemoglobin concentration in *Trp53*$^{\Delta CTD/\Delta CTD}$ animals at P10.

count, *Trp53*$^{\Delta CTD/\Delta CTD}$ animals showed significant anemia, neutropenia, and thrombocytopenia (Fig. 2E). None of these defects were observed in the *Trp53*$^{\Delta CTD/+}$ heterozygous animals.

The terminal 24 amino acids of p53 do not include the tetramerization domain (amino acids 307–355). It is therefore likely that wild-type p53 and p53$^{\Delta CTD}$ are capable of co-oligomerization. In order to discern whether the FL p53 protein was playing a dominant-negative role in *Trp53*$^{\Delta CTD/+}$ mice, these animals were crossed with *Trp53*$^{-/-}$ mice. The *Trp53*$^{\Delta CTD/-}$ offspring were phenotypically indistinguishable from *Trp53*$^{\Delta CTD/+}$, *Trp53*$^{+/-}$, and *Trp53*$^{-/-}$ animals up to 10 mo of age (data not shown). In contrast to *Trp53*$^{-/-}$ animals, which succumb to spontaneous lymphomas or sarcomas 6 mo after birth, *Trp53*$^{\Delta CTD/+}$ and *Trp53*$^{\Delta CTD/-}$ mice were all tumor-free up to the age of 6 mo (data not shown). Thus, the truncated mutant p53 retains tumor suppressor activity. The rescue of *Trp53*$^{\Delta CTD/\Delta CTD}$ mice by deletion of one of the mutant alleles (Fig. 2C) also supports the idea that the level and/or activity of the p53 protein devoid of its C terminus (p53$^{\Delta CTD}$) are central to the observed phenotype.

Deletion of the C-terminal 24 amino acids from p53 induces hematopoietic failure post-partum

To investigate this further, histopathology studies using paraffin sections of P10 pups were conducted. No significant differences were observed in kidney, bladder, skin, or lungs at P10 (Supplemental Fig. 2C; data not shown). The hematopoietic compartment, however, was strongly affected by the deletion of the C terminus. Although no significant differences between genotypes were observed immediately before birth (E18.5) in bone marrow (Fig. 3A) and liver (Fig. 3B), *Trp53*$^{\Delta CTD/\Delta CTD}$ bone marrow cellularity started to decline as early as P1 and was virtually

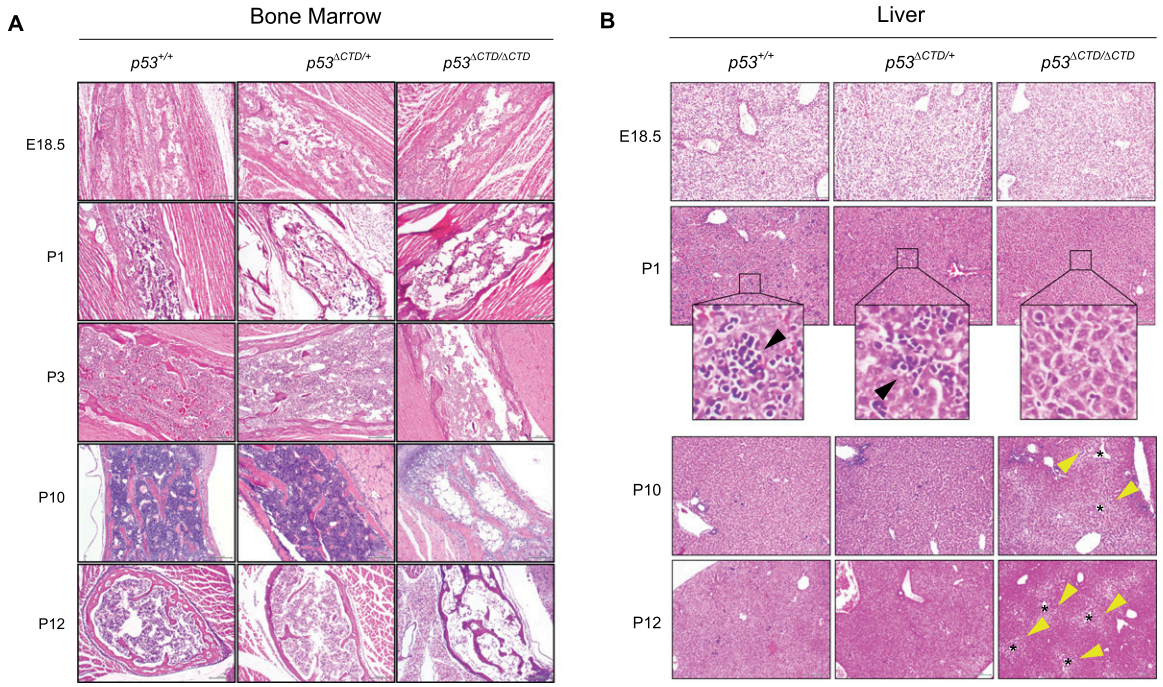

Figure 3. Deletion of the C-terminal 24 amino acids from p53 induces hematopoietic failure post-partum. (*A*) Bone sections stained with haematoxylin and eosin (H&E) from *Trp53*$^{+/+}$, *Trp53*$^{\Delta CTD/+}$, and *Trp53*$^{\Delta CTD/\Delta CTD}$ animals of the indicated ages. No difference is observed at E18.5 among all phenotypes, but a progressive hematopoietic failure is seen as soon as P1 only in *Trp53*$^{\Delta CTD/\Delta CTD}$ animals. (*B*) Liver sections stained with H&E show no difference between E18.5 *Trp53*$^{+/+}$, *Trp53*$^{\Delta CTD/+}$, and *Trp53*$^{\Delta CTD/\Delta CTD}$ animals and an impaired EMH (indicated by black arrowheads) starting as soon as P1 only in *Trp53*$^{\Delta CTD/\Delta CTD}$ animals. Centrilobular degeneration (yellow arrowheads) is observed over the regions surrounding the central vein (black asterisks). Bar, 200 μm.

aplastic at P10 or P12 compared with its wild-type and heterozygous counterparts. No difference was noted between the bone marrow of *Trp53*$^{+/+}$ and *Trp53*$^{\Delta CTD/+}$ animals at any age.

Mice normally experience extramedullary hematopoiesis (EMH) in the liver at birth (Wolber et al. 2002), and it ceases around P9–P13. At E18.5, livers from all three genotypes exhibited abundant EMH, characterized by aggregates of mature and immature hematopoietic cells from all three lineages (erythrocytic, granulocytic, and megakaryocytic) (Fig. 3B). At P1, abundant EMH was still apparent in the *Trp53*$^{+/+}$ mouse, with decreased amounts in the *Trp53*$^{\Delta CTD/\Delta CTD}$ mouse (Fig. 3B). At P10 and P12, scattered EMH was still present in the *Trp53*$^{+/+}$ and *Trp53*$^{\Delta CTD/+}$ mice, but EMH was virtually absent in the *Trp53*$^{\Delta CTD/\Delta CTD}$ mice. There was also centrilobular vacuolar degeneration in the *Trp53*$^{\Delta CTD/\Delta CTD}$ mice at P10 and P12 that was not apparent in the *Trp53*$^{+/+}$ and *Trp53*$^{\Delta CTD/+}$ mice (Fig. 3B). Centrilobular areas are the last to receive oxygenated blood in the liver and are more susceptible to hypoxic injury. The *Trp53*$^{\Delta CTD/\Delta CTD}$ mice are significantly anemic, and their attendant hypoxia might contribute to the observed centrilobular vacuolar degeneration.

The remaining hematopoietic organs were also affected by the deletion of the C terminus of p53. The spleens of *Trp53*$^{+/+}$ and *Trp53*$^{\Delta CTD/+}$ mice were identical in size and cellularity (Figs. 2D, 9C, below) and exhibited abundant EMH in the red pulp and cellular white pulp. The spleens of the *Trp53*$^{\Delta CTD/\Delta CTD}$ mice, in contrast, were dramatically reduced in size and cellularity (Figs. 2D, 9C, below) and exhibited sparse EMH and less cellular white pulp (Fig. 9C, below). Likewise, although no differences were noted between the *Trp53*$^{+/+}$ and *Trp53*$^{\Delta CTD/+}$ mice, the thymus was markedly less cellular in the *Trp53*$^{\Delta CTD/\Delta CTD}$ mice, especially prominent in the cortex (Fig. 6C, below). Gut-associated lymphoid tissue (GALT) and lymph nodes were not apparent in most of the *Trp53*$^{\Delta CTD/\Delta CTD}$ mice, and when present, these tissues were much less cellular than their *Trp53*$^{+/+}$ and *Trp53*$^{\Delta CTD/+}$ counterparts (Supplemental Fig. 2C). Taken together, these data argue that the deletion of the C terminus of p53 has profound consequences for both medullary hematopoiesis and EMH.

Hematopoietic failure can have multiple causes but is often associated with hematopoietic stem cell (HSC) defects. To determine whether the C terminus of p53 played a role in HSC functions, the relative abundance of lineage-negative Lin$^-$ Sca1$^+$ cKit$^+$ (LSK) cells (in prenatal livers and P10 whole bone marrow) of *Trp53*$^{+/+}$, *Trp53*$^{\Delta CTD/+}$, *Trp53*$^{\Delta CTD/\Delta CTD}$, and *Trp53*$^{-/-}$ mice was measured by flow cytometry. Although no significant difference was observed in the relative frequency of LSK cells between the *Trp53*$^{+/+}$, *Trp53*$^{\Delta CTD/+}$, and *Trp53*$^{\Delta CTD/\Delta CTD}$ mice in the fetal liver at E14.5 (Fig. 4A; Supplemental Fig. 3A), a statistically significant reduction in the absolute number of fetal liver LSK cells was noted in the *Trp53*$^{\Delta CTD/\Delta CTD}$ mice. In accordance with previous studies, the relative numbers of LSK cells were higher in *Trp53*$^{-/-}$ mice. By comparison, in the whole bone marrow at P10, both the relative

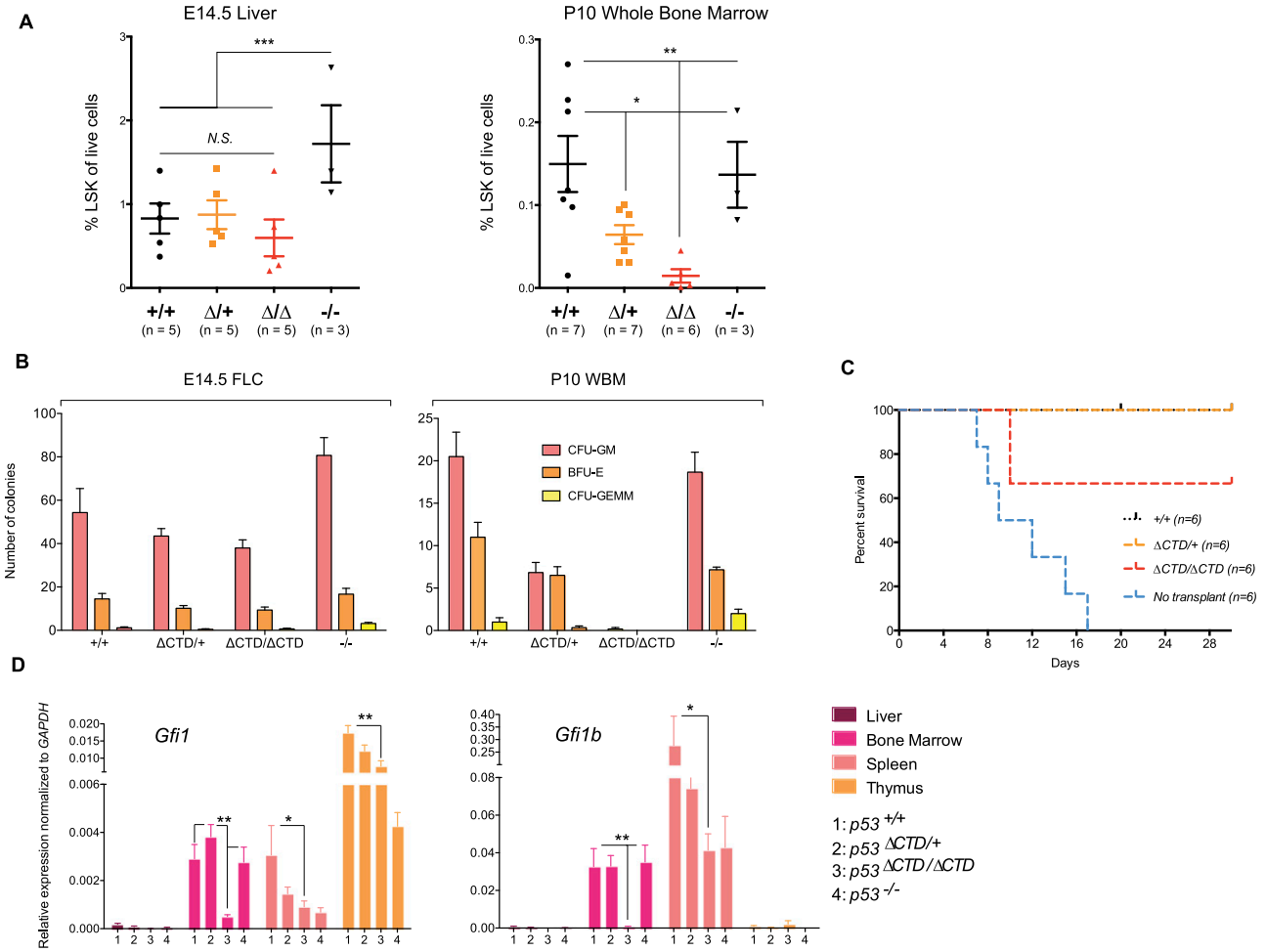

Figure 4. HSC homeostasis is perturbed in *Trp53*$^{\Delta CTD/\Delta CTD}$ mice. (*A*) Percentages of LSK cells from E14.5 fetal liver and P10 whole bone marrow show decreased numbers of HSCs in the bone marrow. Bars indicate SEM. (*) $P < 0.05$; (**) $P < 0.01$; (***) $P < 0.001$ (one-way ANOVA); (N.S.) nonsignificant. (*B*) Number of colonies formed by E14.5 fetal liver and P10 whole bone marrow cells from *Trp53*$^{+/+}$, *Trp53*$^{\Delta CTD/+}$, *Trp53*$^{\Delta CTD/\Delta CTD}$, and *Trp53*$^{-/-}$ animals cultivated on methylcellulose-based medium. Colonies originating from three types of progenitors were counted: erythroid progenitors (burst-forming unit-erythroid [BFU-E]), granulocyte and macrophage progenitors (colony-forming unit-granulocyte and macrophage [CFU-GM]), and multipotential granulocyte, erythroid, macrophage, and megakaryocyte progenitors (CFU-granulocyte, erythroid, macrophage, and megakaryocyte [CFU-GEMM]). (*C*) The percentage survival of lethally irradiated mice of mixed genetic background (BL6/129Sv) transplanted with E14.5 fetal liver cells from matching BL6/129Sv *Trp53*$^{+/+}$, *Trp53*$^{\Delta CTD/+}$, and *Trp53*$^{\Delta CTD/\Delta CTD}$ embryos shows the decreased ability of ΔCTD/ΔCTD cells to recolonize the recipient bone marrow. Animals receiving no transplant were used as negative control. (*D*) Relative expression of two transcription factors essential for hematopoiesis (*Gfi1* and *Gfi1b*) in P10 livers, bone marrow, spleens, and thymi from *Trp53*$^{+/+}$, *Trp53*$^{\Delta CTD/+}$, *Trp53*$^{\Delta CTD/\Delta CTD}$, and *Trp53*$^{-/-}$ animals by qRT–PCR reveals impaired activity for the p53ΔCTD mutant. Expression is normalized to *Gapdh*. In all panels, $n = 5$; bars indicate SEM; (*) $P < 0.05$; (**) $P < 0.01$ (Student's *t*-test).

frequency and absolute numbers of LSK cells were significantly decreased in the *Trp53*$^{\Delta CTD/+}$ and *Trp53*$^{\Delta CTD/\Delta CTD}$ mice in a dose-dependent manner (Fig. 4A; Supplemental Fig. 3B). In fact, the LSK population in the bone marrow of the *Trp53*$^{\Delta CTD/\Delta CTD}$ mice was nearly completely depleted. (Fig. 4A; Supplemental Fig. 3B). To compare the differentiation capacity of stem cells from the wild-type and mutant fetal liver and P10 bone marrow, a colony-forming unit assay was conducted. Interestingly, in accordance with the measurable presence of LSK cells by flow cytometry in the livers of the *Trp53*$^{\Delta CTD/\Delta CTD}$ mice, the liver cells cultured from the *Trp53*$^{+/+}$, *Trp53*$^{\Delta CTD/+}$, and *Trp53*$^{\Delta CTD/\Delta CTD}$ mice were capable of forming colonies (Fig. 4B), implying that the differentiation capacity of the *Trp53*$^{\Delta CTD/\Delta CTD}$ liver LSK cells is intact in vitro. Conversely, no colonies were observed using whole bone marrow cells from *Trp53*$^{\Delta CTD/\Delta CTD}$ mice (Fig. 4B; Supplemental Fig. 3C), in accordance with the observed ablation of LSK cells in *Trp53*$^{\Delta CTD/\Delta CTD}$ mouse bone marrow measured by flow cytometry. HSCs are highly sensitive to reactive oxygen species (ROS), which limit and impair their functions (He et al. 2009). It has also been shown that ROS can induce the p53 pathway. Nevertheless, cultivating the fetal liver cells in 5% oxygen did not rescue the phenotype observed at 20% oxygen (data not shown).

To address whether the wild-type or mutant HSC repopulating capabilities were different, fetal liver cells from donor mice with varying genotypes (+/+, ΔCTD/+, or ΔCTD/ΔCTD) were transplanted into lethally irradiated recipient mice of matching mixed genetic background (BL6/129Sv). Less than 70% of the recipients who received either ΔCTD/ΔCTD cells survived, (Fig. 4C), demonstrating that the HSCs from the *Trp53*$^{\Delta CTD/\Delta CTD}$ fetal livers are capable of reconstituting the bone marrow of the irradiated recipient, although not as consistently as their wild-type counterparts. This capacity to reconstitute the wild-type recipient mice is in accordance with the in vitro colony-forming capacity of the *Trp53*$^{\Delta CTD/\Delta CTD}$ fetal liver cells (Fig. 4B). The reduced ability to reconstitute all irradiated recipients may indicate a cell-intrinsic defect in the *Trp53*$^{\Delta CTD/\Delta CTD}$ HSCs or simply reflect the reduced absolute LSK cell numbers among mutant fetal liver cells. These data collectively demonstrate that the deletion of the C terminus of p53 disturbs critical HSC functions, including differentiation and repopulating capacities.

Recent studies have shown that p53 plays a pivotal role in HSC self-renewal (Milyavsky et al. 2010) and quiescence (Liu et al. 2009), in part by activating a subset of specific and relevant target genes. Notably, p53 transcriptionally activates expression of the transcription factor Gfi1, which has been shown with its homolog, Gfi1b, to be one of the key regulators of hematopoiesis (Cellot and Sauvageau 2005; Duan and Horwitz 2005; Liu et al. 2009; van der Meer et al. 2010). *Gfi1* and *Gfi1b* are both expressed in a tissue-specific manner. Although both are expressed in the bone marrow, *Gfi1* is expressed exclusively in the thymus, while *Gfi1b* is expressed in the spleen (Tong et al. 1998). The expression levels of these genes in hematopoietic tissues across different genotypes were measured by quantitative RT–PCR (qRT–PCR) (Fig. 4D). Interestingly, basal levels of *Gfi1* were controlled by p53 only in the thymus (Fig. 4D) and to a lesser extent in the spleen, even though the overall expression in the latter was significantly diminished compared with the thymus, as expected. In the bone marrow, on the other hand, *Gfi1* basal levels were identical between *Trp53*$^{+/+}$, *Trp53*$^{\Delta CTD/+}$, and *Trp53*$^{-/-}$ genotypes but were significantly reduced in the *Trp53*$^{\Delta CTD/\Delta CTD}$ animals. The same pattern was observed for *Gfi1b*, with p53 controlling basal levels of *Gfi1b* in the spleen but not in the bone marrow (Fig. 4D). Thus, in the bone marrow, the dominant source of hematopoiesis in newborn and adult mice, the deletion of the C terminus of p53 resulted in reduced expression of *Gfi1* and *Gfi1b*, two of the most important regulators of hematopoietic homeostasis. These low levels of *Gfi1* and *Gfi1b* might indicate that the pool of cells in which these two genes are normally expressed is absent in the mutant bone marrow. Furthermore, flow cytometric analysis of CD3$^+$, CD19$^+$, and CD11b$^+$ populations revealed an aberrant cellular subset composition in the mutant bone marrow, with an accumulation of CD3-positive cells and no change in CD19$^+$ or CD11b$^+$ cells' relative frequency among all genotypes (Supplemental Fig. 7). It is also possible that abnormal expression of p53 target genes within different hematopoietic lineages may drive shifts in cell populations within organs, which may account for differences in whole-tissue gene expression readouts. This could explain, at least in part, the phenotypic difference observed between *Trp53*$^{-/-}$ and *Trp53*$^{\Delta CTD/\Delta CTD}$ mice and the hematopoietic failure observed in the latter after birth.

Deletion of the C-terminal 24 amino acids from p53 induces senescence in bone marrow cells

To gain further insight into the mechanism of hematopoietic failure in *Trp53*$^{\Delta CTD/\Delta CTD}$ mice, p53-dependent senescence and apoptosis were assessed in whole bone marrow cells isolated from P10 animals. First, whole bone marrow cells from P10 animals were stained for senescence-associated β-galactosidase (SA-β-Gal) activity (Fig. 5A,B). The number of SA-β-Gal-positive cells was greatly increased in *Trp53*$^{\Delta CTD/\Delta CTD}$ animals, while little was observed between the other genotypes. mRNA levels of several bona fide senescence markers were measured by qRT–PCR. *Cdkn1a* (p21) and *Cdkn2b* (p15^{INK4b}), two potent cell cycle inhibitors that have been shown to be overexpressed in senescent cells (Collado and Serrano 2006), were up-regulated in the mutant bone marrow cells (Fig. 5C). Expression of *Cdkn1a* (p21) is clearly p53-dependent, as its level is markedly reduced in p53-null tissue. The increase in its expression is thus likely due to hyperactivity of p53$^{\Delta CTD}$. This was not the case for several other p53 target genes, including *Mdm2*, *Bbc3* (Puma), *Pmaip1* (Noxa), or *Tigar* (Supplemental Fig. 4). Expression of *Cdkn2b* (p15^{INK4b}) is also similar between wild-type and null animals. Thus, in the case of *Cdkn2b* (p15^{INK4b}), the increased levels that are observed (Fig. 5C) are likely an indicator of the enhanced senescence. Two other transcripts originating from the *Cdkn2a* locus (p19^{ARF} and p16^{INK4a}) did not show any statistically significant difference between *Trp53*$^{+/+}$, *Trp53*$^{\Delta CTD/+}$, *Trp53*$^{\Delta CTD/\Delta CTD}$, and *Trp53*$^{-/-}$ bone marrow. In addition, bone marrow cells were stained for activated caspase 3, an apoptotic marker (Fig. 5D). MEFs derived from *Trp53*$^{+/+}$, *Trp53*$^{\Delta CTD/+}$, *Trp53*$^{\Delta CTD/\Delta CTD}$, and *Trp53*$^{-/-}$ E14.5 embryos and treated with the DNA-damaging agent DOX for 24 h were used as positive and negative controls (Fig. 5D, inserts). Although the p53$^{\Delta CTD}$ mutant protein retained its ability to induce apoptosis after DNA damage in these cells, no apoptosis was observed in bone marrow cells from all of the genotypes tested (Fig. 5D). These data suggest that although p53$^{\Delta CTD}$ retains its ability to induce both senescence and apoptosis, only senescence is involved in the observed bone marrow phenotype.

In the thymus, the C-terminal domain negatively regulates p53-dependent gene expression by inhibiting DNA binding

The thymi in the *Trp53*$^{\Delta CTD/\Delta CTD}$ mice are reduced in size (Fig. 2D) and show severe morphological differences at the microscopic level (Fig. 6C). To examine p53-dependent effects in this tissue, the gene expression of a set of well-characterized p53 targets was compared

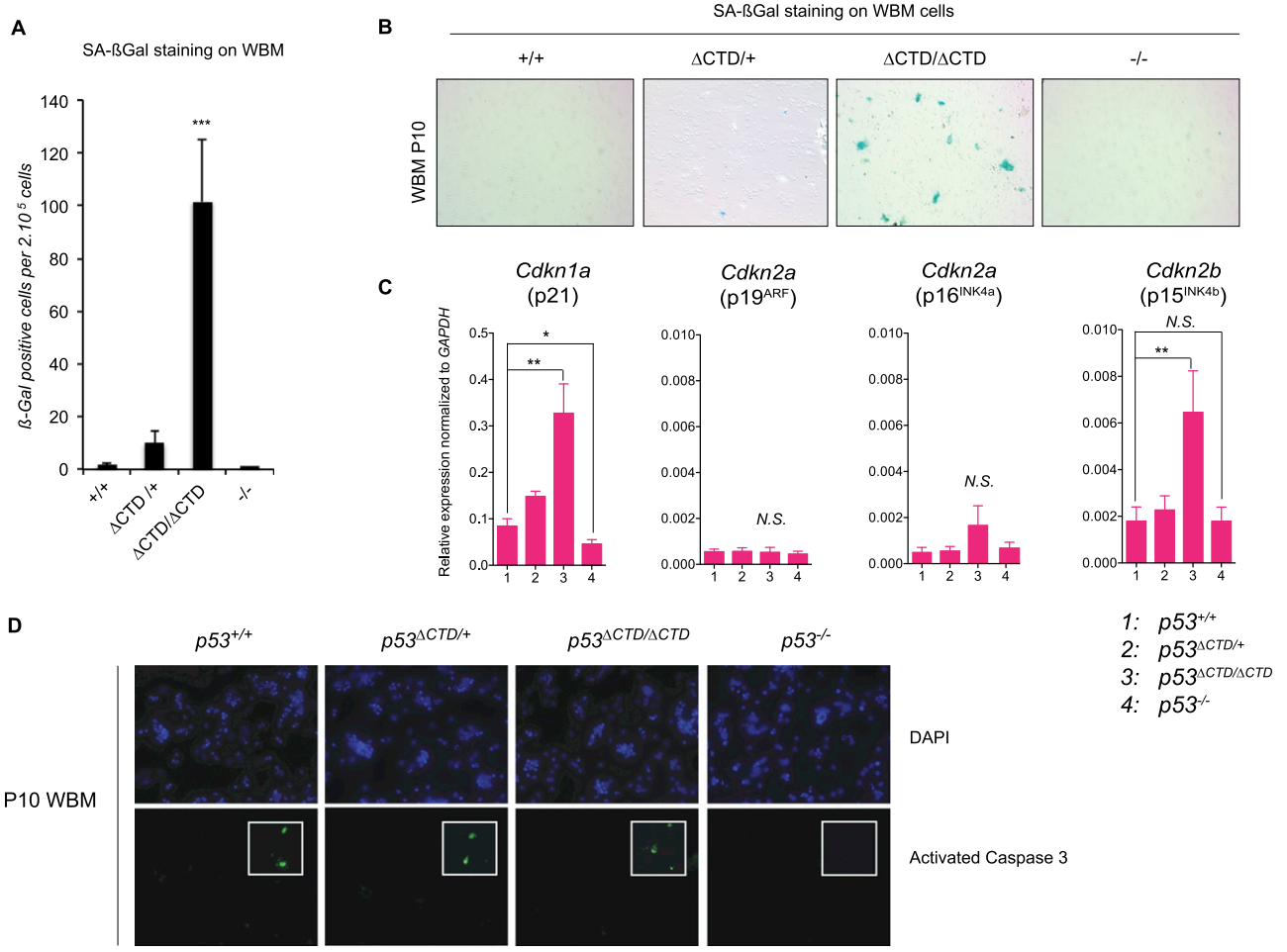

Figure 5. Deletion of the C-terminal 24 amino acids from p53 induces senescence in bone marrow cells. (*A*) Quantitative assay of SA-β-Gal activity in P10 bone marrow cells from *Trp53*$^{+/+}$, *Trp53*$^{\Delta CTD/+}$, *Trp53*$^{\Delta CTD/\Delta CTD}$, and *Trp53*$^{-/-}$ animals reveals a marked increase in senescent cells in the mutant bone marrow. $n = 5$; bars indicate SEM; (***) $P < 0.001$ (Student's *t*-test). (*B*) Representative pictures of *A*. (*C*) Relative expression of several senescence markers in P10 whole bone marrow from *Trp53*$^{+/+}$, *Trp53*$^{\Delta CTD/+}$, *Trp53*$^{\Delta CTD/\Delta CTD}$, and *Trp53*$^{-/-}$ animals by qRT–PCR. The p53 direct target gene *Cdkn1a* (p21) is a bona fide senescence marker and is up-regulated in ΔCTD/ΔCTD bone marrow. *Cdkn2b* but not the two transcripts encoded by *Cdkn2a* is significantly up-regulated in the ΔCTD/ΔCTD bone marrow. Expression is normalized to *Gapdh*. In all panels, $n = 5$; bars indicate SEM; (*) $P < 0.05$; (**) $P < 0.01$ (Student's *t*-test); (N.S.) nonsignificant. (*D*) Whole bone marrow cells from P10 animals of the genotypes *Trp53*$^{+/+}$, *Trp53*$^{\Delta CTD/+}$, *Trp53*$^{\Delta CTD/\Delta CTD}$, and *Trp53*$^{-/-}$ stained with an activated caspase 3 antibody, a bona fide marker for apoptotic cells, did not show enhanced apoptosis. *Insets* represent MEFs derived from E14.5 *Trp53*$^{+/+}$, *Trp53*$^{\Delta CTD/\Delta CTD}$, and *Trp53*$^{-/-}$ embryos and treated with the DNA-damaging agent DOX at 0.2 μg/mL. Twenty-four hours after treatment, cells were fixed and stained with an anti-activated caspase 3. Unlike p53$^{-/-}$ cells, p53$^{\Delta CTD/\Delta CTD}$ MEFs are capable of undergoing apoptosis after DNA damage to the same extent as p53$^{+/+}$ or p53$^{\Delta CTD/+}$ MEFs.

between wild-type and p53-null animals (Fig. 6A). All targets examined showed clear p53 dependence in their gene expression: *Cdkn1a* (p21), *Mdm2*, *Bbc3* (Puma), *Pmaip1* (Noxa), and *Tigar* (Fig. 6A). Of these, the wild-type and the p53$^{\Delta CTD}$ mice showed little difference in expression of either *Cdkn1a* (p21), *Mdm2*, or *Tigar*. In contrast, both *Bbc3* (Puma) and *Pmaip1* (Noxa) showed significantly increased expression in the presence of the p53$^{\Delta CTD}$. The effects on p21 and Puma protein expression were confirmed by immunoblotting (Fig. 6B). These differences in gene expression were not due to altered p53 levels, determined by either immunoblotting of tissue extracts (Fig. 6B) or immunohistochemistry (IHC) (Fig. 6C). To gain mechanistic insight into the difference in gene expression, chromatin immunoprecipitation (ChIP) analysis was performed on selected genomic sites. Occupancy of p53 on all sites examined was only seen in the wild-type but not the null tissues (Fig. 6D). Although wild-type and p53$^{\Delta CTD}$ were found equivalently associated with the two response elements in the *Cdkn1a* (p21) promoter, the p53$^{\Delta CTD}$ showed markedly increased occupancy on the elements in the *Bbc3* (Puma) and *Pmaip1* (Noxa) genes (Fig. 6D). Thus, the enhanced *Bbc3* (Puma) and *Pmaip1* (Noxa) expression seen with p53$^{\Delta CTD}$ is accompanied by increased occupancy of the relevant genomic sites. This suggests that in the thymus, the C terminus of p53 negatively regulates DNA binding at least on a subset of target genes.

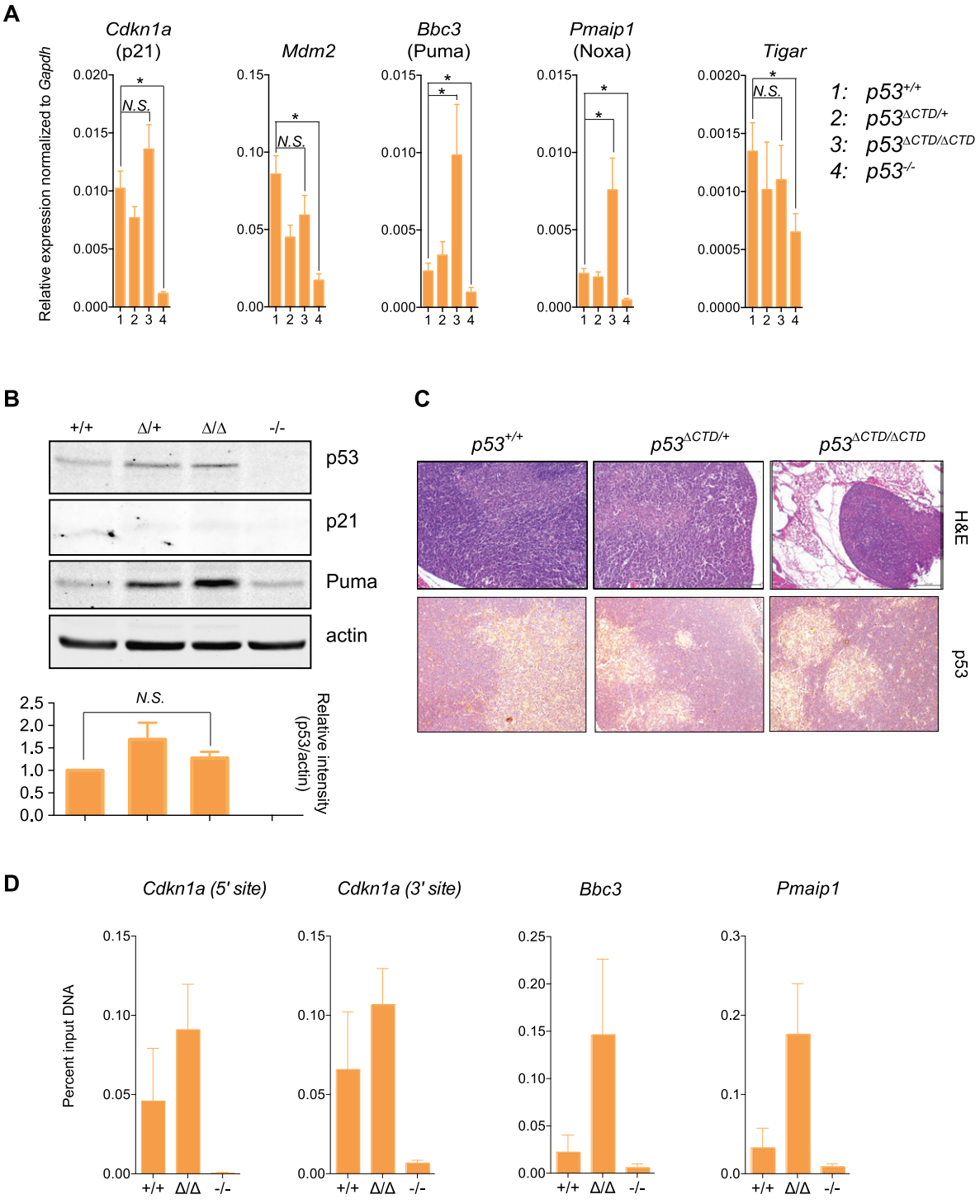

Figure 6. The C-terminal domain is a negative regulator of p53 activity in the thymus. (*A*) Relative expression of five p53 direct target genes in P10 thymi from *Trp53*$^{+/+}$, *Trp53*$^{\Delta CTD/+}$, *Trp53*$^{\Delta CTD/\Delta CTD}$, and *Trp53*$^{-/-}$ animals by qRT–PCR demonstrates tissue-specific up-regulation of the two proapoptotic targets *Bbc3* (Puma) and *Pmaip1* (Noxa). Expression is normalized to *Gapdh*. In all panels, $n = 5$; bars indicate SEM; (*) $P < 0.05$ (Student's *t*-test). (*B*, *top*) Immunoblot shows comparable p53 expression between the wild-type and mutant thymi at P10. p21 expression is not changed, whereas Puma protein levels are increased in the mutant thymus. β-Actin was used as the loading control. (*Bottom*) Quantitation of p53 levels (relative intensity of p53 bands vs. actin bands), $n = 5$; bars indicate SEM; (P) Student's *t*-test; (N.S.) nonsignificant. (*C*) P10 *Trp53*$^{\Delta CTD/\Delta CTD}$ thymi display reduced size and cellularity but no difference in basal p53 levels, as assessed by H&E staining and IHC, respectively. Bar, 200 μm. (*D*) ChIP on P10 thymus protein extracts followed by qPCR demonstrates enhanced binding of p53$^{\Delta CTD}$ on its response elements within *Bbc3* (Puma) and *Pmaip1* (Noxa) genes.

Hyperactive p53 lacking the C-terminal domain induces apoptosis but not senescence in thymocytes

To determine whether this enhanced expression of pro-apoptotic targets has a corresponding phenotypic outcome, thymocytes were stained for either SA-β-Gal activity (as a marker for senescence) or activated (cleaved) caspase 3 (as an indicator of apoptosis) (Fig. 7). Although little SA-β-Gal activity could be detected (Fig. 7B), there is clear evidence of activated caspase 3 in the thymi from ΔCTD/ΔCTD mice but not those harvested from either the wild-type or heterozygous animals (Fig. 7A). Taken together, this indicated that in the thymus, the C terminus of p53 prevents DNA binding to *Bbc3* (Puma) and *Pmaip1* (Noxa) but not *Cdkn1a* (p21). This in turn leads to differential gene expression that is consistent with an enhanced apoptosis in these tissues. It is likely, then, that this increased cell death is responsible for the smaller thymus size in the homozygous mutant mice.

In the liver, the C-terminal domain of p53 is required for target gene expression at a step subsequent to DNA binding

Livers from the *Trp53*$^{\Delta CTD/\Delta CTD}$ mice are unaffected in size (Fig. 2D) but show altered colorization, most likely due to altered blood cell production (Fig. 2E). To examine p53-dependent effects in this tissue, p53 target gene expression was again compared between wild-type and p53-null animals (Fig. 8A). *Cdkn1a* (p21), *Mdm2*, *Pmaip1* (Noxa), and *Tigar* showed clear p53 dependence in their gene expression, while *Bbc3* (Puma) did not (Fig. 8A). As in the thymus, comparison of wild-type and p53$^{\Delta CTD}$ mice showed little difference in expression of *Cdkn1a* (p21). In contrast, *Mdm2*, *Pmaip1* (Noxa), and *Tigar* all showed significantly reduced expression in the presence of the p53$^{\Delta CTD}$. The effects on p21 protein expression were confirmed by immunoblotting (Fig. 8B). These differences in gene expression were not due to altered p53 levels, determined by either immunoblotting of tissue extracts (Fig. 8B) or IHC (Fig. 8C). ChIP analysis showed that occupancy of p53 on all sites examined was only seen in the wild-type but not the null tissues (Fig. 8D). There were no significant differences in promoter occupancy by wild type or p53$^{\Delta CTD}$ for either the *Cdkn1a* (p21), *Mdm2*, or *Pmaip1* (Noxa) genes (Fig. 8D). Intriguingly, the p53$^{\Delta CTD}$ showed markedly reduced occupancy on the *Tigar* gene (Fig. 8D). Thus, the reduced gene expression seen with p53$^{\Delta CTD}$ is not reflected in changes in occupancy of the relevant genomic sites. This argues that in the liver, the C terminus of p53 is needed for a subsequent step in transcriptional regulation beyond DNA binding, perhaps at the level of coactivator recruitment.

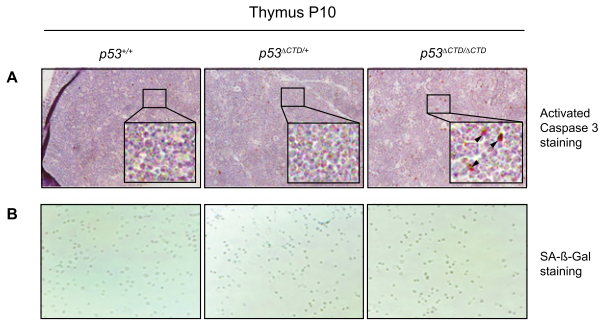

Figure 7. Hyperactive p53 lacking the C-terminal domain induces apoptosis but not senescence in thymocytes. (*A*) IHC on thymus sections from P10 *Trp53*$^{+/+}$, *Trp53*$^{\Delta CTD/+}$, and *Trp53*$^{\Delta CTD/\Delta CTD}$ animals reveals a significant increase of activated caspase 3 staining in the mutant thymus. Black arrowheads show activated caspase 3-positive cells. (*B*) SA-β-Gal activity in P10 thymocytes isolated from *Trp53*$^{+/+}$, *Trp53*$^{\Delta CTD/+}$, and *Trp53*$^{\Delta CTD/\Delta CTD}$ animals reveals no difference in the number of senescent cells between wild-type, heterozygous, or homozygous mutant thymi.

In the spleen, p53 lacking the C-terminal domain is hyperactive due to its overexpression

Spleens from the *Trp53*$^{\Delta CTD/\Delta CTD}$ mice are reduced in size (Fig. 2D) and show morphological differences at the microscopic level (Fig. 9C). In this tissue, p53-dependent expression of *Cdkn1a* (p21), *Pmaip1* (Noxa), and *Tigar* is seen, but not for *Mdm2* or *Bbc3* (Puma) (Fig. 9A). Mice expressing p53$^{\Delta CTD}$ showed enhanced expression of *Cdkn1a* (p21) and *Pmaip1* (Noxa) but reduced mRNA levels of *Tigar* (Fig. 9A). The effects on p21 protein expression were confirmed by immunoblotting (Fig. 9B). In contrast to the thymus and liver, p53$^{\Delta CTD}$ levels were substantially higher, as seen by immunoblotting of tissue extracts (Fig. 9B) or IHC (Fig. 9C). There was no detectable evidence of senescence or apoptosis using appropriate assays (Fig. 9D). Thus, the increased protein levels of p53$^{\Delta CTD}$ are accompanied by enhanced gene expression on some (*Cdkn1a* and *Pmaip1*) but not other (*Tigar*) genes. The molecular basis for this striking difference remains to be determined. p53$^{\Delta CTD}$ is similarly overexpressed in fetal livers (Supplemental Fig. 5A,B). As in the spleen, this is accompanied by enhanced gene expression of *Cdkn1a* (p21) and *Pmaip1* (Noxa) and reduced levels of *Tigar* mRNA (Supplemental Fig. 5C). In contrast to the thymus and adult liver, in the spleen and fetal liver, the C terminus is needed to maintain appropriate p53 protein levels.

The p53 C-terminal domain is required for proper cerebellum development in vivo

Aside from hematopoietic failure, another major phenotype observed in *Trp53*$^{\Delta CTD/\Delta CTD}$ mice was pronounced ataxia, which suggested the presence of neurological defects. Thus, the brains of *Trp53*$^{+/+}$ and *Trp53*$^{\Delta CTD/\Delta CTD}$ animals were compared. Overall, the brains of homozygous mutant mice were smaller than those of their wild-type or heterozygous counterparts (Supplemental Fig. 6A; data not shown). The cerebellar vermis in the homozygous mutant brain was virtually nonexistent, revealing more of the colliculi (Supplemental Fig. 6A). In addition, the cerebellar folia appeared shallower with a perturbed foliation pattern, while no significant differences were noted in the cerebrum or brainstem (Supplemental Fig. 6B). Previous studies have shown that p53 levels are

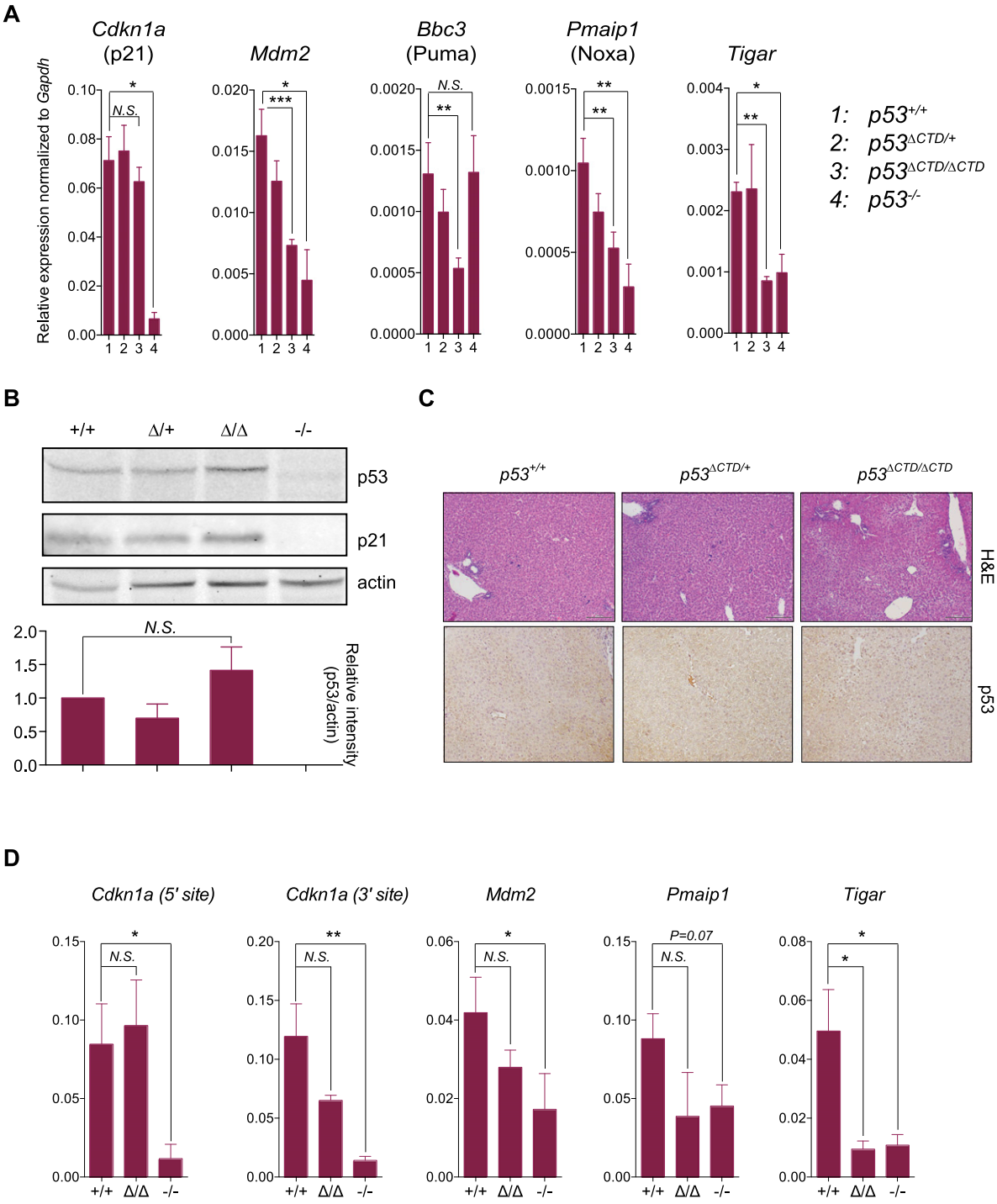

Figure 8. In the liver, p53 lacking the C-terminal domain is expressed at wild-type levels but is defective in gene expression. (*A*) Relative expression of five p53 direct target genes in P10 livers from *Trp53*$^{+/+}$, *Trp53*$^{\Delta CTD/+}$, *Trp53*$^{\Delta CTD/\Delta CTD}$, and *Trp53*$^{-/-}$ animals by qRT–PCR demonstrates tissue-specific down-regulation of all targets except p21. Expression is normalized to *Gapdh*. In all panels, n = 5; bars indicate SEM; (*) $P < 0.05$; (**) $P < 0.01$; (***) $P < 0.001$; (N.S) nonsignificant (Student's t-test). (*B*, *top*) Immunoblot shows comparable p53 expression between wild-type and mutant livers at P10. β-Actin was used as the loading control. (*Bottom*) Quantitation of p53 levels (relative intensity of p53 bands vs. actin bands); n = 5; bars indicate SEM; (P) Student's t-test; (N.S.) nonsignificant. (*C*) P10 *Trp53*$^{+/+}$ and *Trp53*$^{\Delta CTD/\Delta CTD}$ livers display comparable size and cellularity and no difference in basal p53 levels, as assessed by H&E staining and IHC, respectively. Bar, 200 μm. (*D*) ChIP on P10 liver protein extracts followed by qPCR. In all panels, n = 4; bars indicate SEM; (*) $P < 0.05$; (**) $P < 0.01$; (N.S.) nonsignificant (Student's t-test).

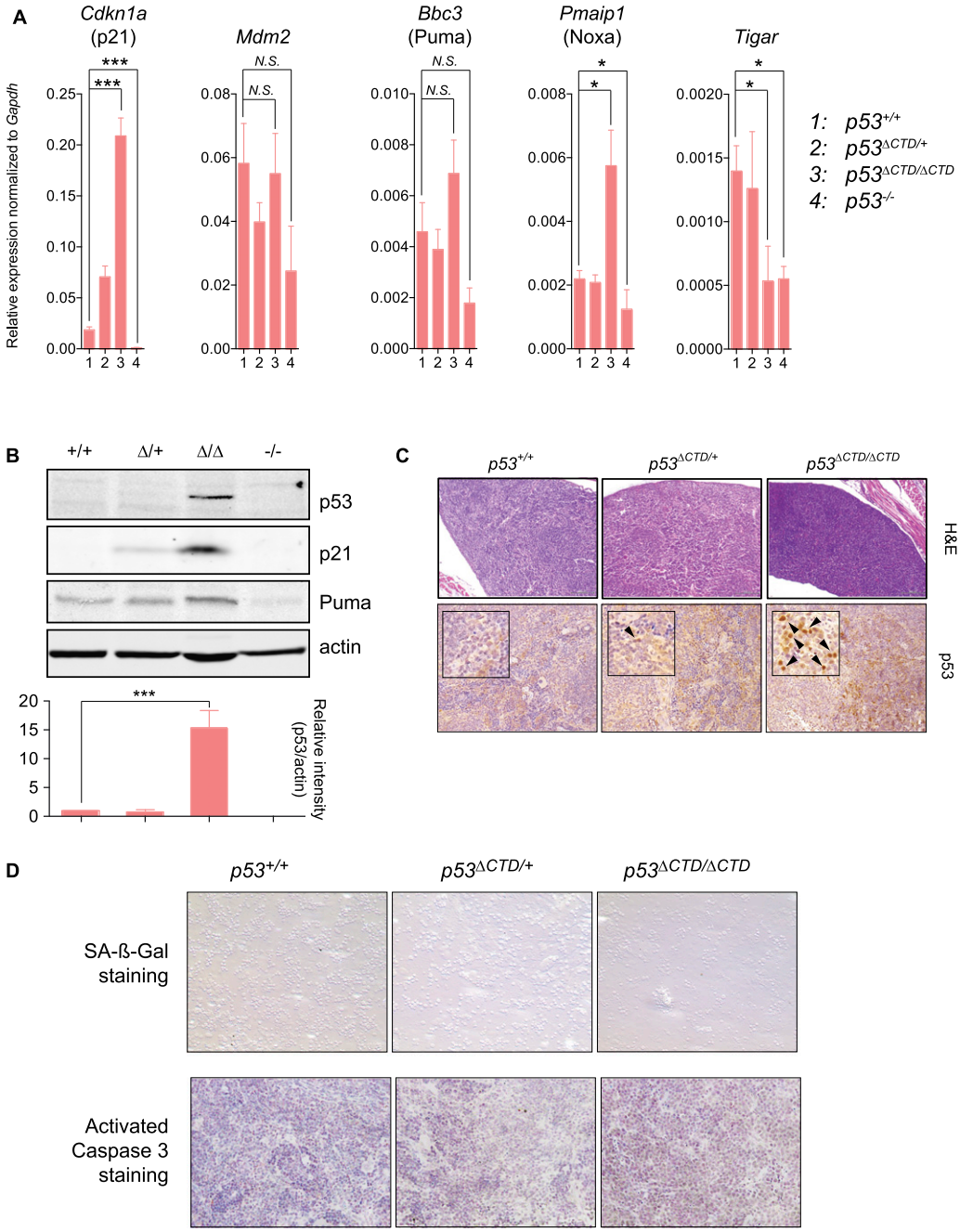

Figure 9. In the spleen, p53 lacking the C-terminal domain is overexpressed and hyperactive in a target gene-selective manner. (*A*) Relative expression of five p53 direct target genes in P10 spleens from *Trp53*$^{+/+}$, *Trp53*$^{\Delta CTD/+}$, *Trp53*$^{\Delta CTD/\Delta CTD}$, and *Trp53*$^{-/-}$ animals by qRT–PCR demonstrates target-specific regulation. Expression is normalized to *Gapdh*. In all panels, $n = 5$; bars indicate SEM; (*) $P < 0.05$; (***) $P < 0.001$; (N.S.) nonsignificant (Student's *t*-test). (*B*, *top*) Immunoblot shows increased p53 expression in the mutant spleen compared with wild type at P10. β-Actin was used as the loading control. (*Bottom*) Quantitation of p53 levels (relative intensity of p53 bands vs. actin bands); $n = 5$; bars indicate SEM; (***) $P < 0.001$ (Student's *t*-test). (*C*) Histology of the spleen of P10 animals shows no difference between *Trp53*$^{+/+}$ and *Trp53*$^{\Delta CTD/+}$ organs but reduced size and cellularity in *Trp53*$^{\Delta CTD/\Delta CTD}$ animals. IHC on the same tissues reveals a significant and dose-dependent increase of p53 protein expression. Bar, 200 μm. (*D*, *top*) SA-β-Gal activity in P10 splenocytes isolated from *Trp53*$^{+/+}$, *Trp53*$^{\Delta CTD/+}$, and *Trp53*$^{\Delta CTD/\Delta CTD}$ animals reveals no difference in senescent cell numbers between wild-type, heterozygous, or mutant thymi. (*Bottom*) IHC on spleen sections from P10 *Trp53*$^{+/+}$, *Trp53*$^{\Delta CTD/+}$, and *Trp53*$^{\Delta CTD/\Delta CTD}$ animals reveals no significant increase of activated caspase 3 staining in the mutant spleen.

critical in the development of the external granular layer (EGL) and internal granular layer (IGL) of the cerebellum (Malek et al. 2011). Accordingly, there was an apparent decrease in the thickness and cellularity of both the EGL and IGL of the *Trp53*$^{\Delta CTD/\Delta CTD}$ cerebellum compared with the *Trp53*$^{+/+}$ and *Trp53*$^{\Delta CTD/+}$ counterparts (Supple-

mental Fig. 6B,C). Of note, the Purkinje cells of the homozygous mutant cerebellum failed to form a uniform monolayer, as observed in the wild-type or heterozygous counterparts (Supplemental Fig. 6C). Interestingly, when assessed by immunoblot, p53 protein levels were increased in the cortex of both $Trp53^{\Delta CTD/+}$ and $Trp53^{\Delta CTD/\Delta CTD}$ animals compared with $Trp53^{+/+}$, whereas no difference was observed in the cerebellum of these three genotypes (Supplemental Fig. 6D). This finding argues that the C-terminal domain regulates p53 functions in the cerebellum without interfering with its level of expression. These data collectively demonstrate the importance of C-terminal regulation of p53 in cerebellar development. Further studies will be needed to determine the precise mechanism by which p53 intervenes in this process.

Discussion

The p53 tumor suppressor is a critical mediator of the cellular response to stress and is mutated in >50% of human tumors (Brosh and Rotter 2009). $Trp53^{-/-}$ mice were originally described as developmentally normal but rapidly succumb to spontaneous cancers (mainly lymphomas and sarcomas) within 6–9 mo after birth (Donehower et al. 1992; Jacks et al. 1994). p53 has also been implicated in stem cell maintenance and homeostasis (Zheng et al. 2008; Cicalese et al. 2009; Liu et al. 2009; Spike and Wahl 2011; Bonizzi et al. 2012). These p53 functions may be of particular relevance to tissues that are known to contain a significant pool of adult stem cells (Uccelli et al. 2008; Doulatov et al. 2012;). As p53 has also been shown to regulate reprogramming of somatic cells into induced pluripotent stem cells (iPSCs), these findings argue in support of the idea that one of the roles of p53 is to tightly regulate homeostatic adult tissues. Similarly, p53 has been implicated in brain development (Liu et al. 2007; Terzian et al. 2007; Malek et al. 2011; Mendrysa et al. 2011). Although originally described as developmentally normal, $Trp53^{-/-}$ mice were later shown to have development defects, including impaired maternal reproduction (Hu et al. 2007), aberrant mesenchymal differentiation programs (Molchadsky et al. 2008), and exencephaly (Armstrong et al. 1995; Sah et al. 1995). The molecular basis for these developmental functions of p53 clearly is an important area for further study.

In the present study, it was shown that the deletion of the C-terminal domain of the p53 protein is sufficient to provoke striking postnatal developmental phenotypes in the absence of induced DNA damage, including hematopoietic failure and brain defects. Previous reports of C-terminal $Trp53^{K6R}$ and $Trp53^{7KR}$ mice in which six or seven lysines have been mutated to arginines failed to show any significant phenotype compared with wild type (Feng et al. 2005; Krummel et al. 2005). Recently, however, a re-evaluation of the $Trp53^{7KR}$ mouse revealed that the C-terminal lysines may be important for HSC survival, although this is only revealed after DNA damage-dependent activation (Wang et al. 2011). While the present study was under consideration, Simeonova et al. (2013) reported that mice expressing a truncated p53 lacking the C-terminal 31 amino acids presented a severe aplastic anemia, leading to death within weeks of birth, similar to what was observed with the p53ΔCTD-expressing mice reported here. These findings and the current data support the hypothesis that p53 C-terminal post-translational modifications are likely to be indispensable for proper p53 function and strongly argue for a central role of p53 in the maintenance and homeostasis of the adult hematopoietic compartment through its basic C-terminal domain. This central and novel role for the C terminus is supported by the observation that the hematopoietic phenotype is triggered by the mere deletion of the C terminus of p53 in the absence of genotoxic stress. Moreover, the data presented here shed light on the mechanisms leading to the hematopoietic failure in $Trp53^{\Delta CTD/\Delta CTD}$ animals.

According to these data, p53 activity is critical in regulating hematopoietic homeostasis in vivo, in agreement with several previous studies (Liu et al. 2007, 2009; Abbas et al. 2010; Wang et al. 2011; Ceccaldi et al. 2012). Both fetal and postnatal hematopoietic tissues are affected by the C-terminal deletion, although to differing extents. Although the absolute number of fetal liver HSCs is reduced in the mutant animals, these cells are still capable of properly differentiating and, to a certain extent, reconstituting the bone marrow of lethally irradiated recipients. Flow cytometry analysis of gross $CD3^+$, $CD19^+$, and $CD11b^+$ populations in P10 organs revealed aberrant cellular subset composition in postnatal hematopoietic tissues, with an overall increase in $CD3^+$ T-cell populations and decrease in $CD19^+$ B-cell populations of mutant p53 mice (Supplemental Fig. 7). Consistent with their observed colony-forming capacity (Fig. 4B), p53 mutant HSCs were capable of differentiating toward major lymphoid and myeloid blood lineages, yet subsequent lineage development and/or homeostasis is somehow disrupted. Hematopoiesis fails by P10 in these mutant p53 mice, leading to death within a time frame coincident with the transition from liver to bone marrow-predominated hematopoiesis. HSCs migrate from the fetal liver to the bone marrow niche, which provides the appropriate cellular and molecular microenvironment for their self-renewal and differentiation (Suda et al. 2005). While the bone marrow of the $Trp53^{\Delta CTD/\Delta CTD}$ mice is virtually devoid of HSCs, fetal liver cells from $Trp53^{\Delta CTD/\Delta CTD}$ mice are capable of engrafting and rescuing lethally irradiated recipient mice, although not as efficiently as wild-type cells. These data raise the intriguing possibility that p53 might also play important roles in such non-cell-autonomous functions as formation or maintenance of the bone marrow stem cell niche. The migration of HSCs to the bone marrow as well as the maintenance of the bone marrow stem cell niche are critically dependent on the chemokine CXCL12 (Suda et al. 2005; Ding and Morrison 2013; Greenbaum et al. 2013). As p53 activation has been demonstrated to attenuate cancer cell migration through repression of CXCL12 (Moskovits et al. 2006), it is tempting to speculate that $p53^{\Delta CTD}$ hyperactivity within the bone marrow niche could cause CXCL12 repression, thereby ablating the CXCL12 chemokine gradient and undermining the bone marrow stem cell niche in the

Trp53$^{\Delta CTD/\Delta CTD}$ mice. Further studies will be needed to determine the extent of p53 contribution in these processes.

Mdm2 negatively regulates p53 protein levels through ubiquitination and subsequent proteasomal degradation. Cell-based studies initially demonstrated that the p53 C-terminal lysines are required for this process (Kubbutat et al. 1997, 1998). Studies in vivo later contradicted these results, however, by showing that mutation of these C-terminal lysines that had been shown to be targeted by ubiquitination had no effect on p53 stability (Feng et al. 2005; Krummel et al. 2005). This could reflect species differences between humans and mice as well. Here it is shown that p53$^{\Delta CTD}$ protein levels are differentially regulated in a tissue-specific manner. In the thymus, cerebellum, and adult liver, the wild-type and truncated p53 proteins are expressed at comparable levels. In contrast, in the spleen, brain cortex, and fetal liver, the p53$^{\Delta CTD}$ protein is found at significantly higher levels. This is reminiscent of previous studies showing that in the setting of a hypomorphic Mdm2 (Malek et al. 2011) or haploinsufficiency for Mdm2 and Mdm4 (Terzian et al. 2007), p53 shows tissue-specific hyperactivity in the hematopoietic compartment and the cerebellum. These findings and the current data support a model in which p53 activity is tightly regulated in specific organs through both its C-terminal domain and its negative regulators, Mdm2 and Mdm4. This is corroborated by one study in which the deletion of the C-terminal domain of p53 decreased the Mdm2–p53 interaction (Poyurovsky et al. 2010). Further investigations will clearly be needed to clarify the relationship between p53 and its negative regulators in *Trp53*$^{\Delta CTD/\Delta CTD}$ animals.

Abnormal levels of several relevant markers (including the cell cycle-dependent kinase inhibitors *Cdkn2b*/p15 and *Cdkn1a*/p21, the latter being a direct p53 target gene) are correlated with high levels of senescence in the bone marrow of mutant animals. Previous studies have shown that HSC quiescence is maintained by *Cdkn1a* (p21) (Cheng et al. 2000). These results are substantiated by other studies that have proposed that p53 counteracts stem cell reprogramming by activating a senescence-promoting stress response (Hong et al. 2009; Utikal et al. 2009). Indeed, a similar phenotype was found in mice that express an endogenous mutant p53 (172P) in the absence of Mdm2 (Liu et al. 2007). This particular mutant p53 protein lacks the ability to mediate an apoptotic response but can still up-regulate p21 and cause cell cycle arrest (Ryan and Vousden 1998). This is consistent with the hematopoietic phenotype being mediated through hyperactivity of the p53-dependent cycle arrest pathway via p21. Interestingly, *Cdkn2b* (p15) has been shown to be repressed by Gfi1, and its knockout in mice leads to monocytosis and predisposition to myeloid leukemia (Basu et al. 2009; Bies et al. 2010). In the *Trp53*$^{\Delta CTD/\Delta CTD}$ mice, down-regulation of *Gfi1* in bone marrow cells is correlated with higher expression of *Cdkn2b* (p15) and senescence. It is tempting to speculate that the senescent cells observed in the mutant bone marrow might correspond to HSCs. In fact, the percentage of senescent cells in the *Trp53*$^{\Delta CTD/\Delta CTD}$ bone marrow roughly equals the commonly admitted percentage of stem cells among whole bone marrow cells in mice (~0.05%) (Fig. 5A). Careful analysis of the bone marrow cell composition will be needed to substantiate this hypothesis.

In addition to controlling levels of expression, the C-terminal domain of p53 has been extensively studied in transcriptional regulation (Kruse and Gu 2009). It has alternatively been shown to exert either a negative or positive effect depending on the particular study and conditions (Kruse and Gu 2009; Carvajal and Manfredi 2013). Its highly basic amino acid content is consistent with an interaction with DNA. Indeed, studies have suggested that it can negatively regulate by interfering with sequence-specific DNA binding by the core domain (Hupp et al. 1992; Anderson et al. 1997; Ahn and Prives 2001). Alternatively, it is required to serve as a means for p53 to track along DNA (McKinney et al. 2004). Post-translational modifications within this domain have also been implicated in the binding of specific transcriptional cofactors (Barlev et al. 2001; Mujtaba et al. 2004). Studies with the *Trp53*$^{\Delta CTD/\Delta CTD}$ serve to reconcile these apparently contradictory findings in the literature in that the C terminus appears to mediate each of these effects but in a tissue-specific and target gene-specific manner.

In the thymus, wild-type and truncated p53 are not expressed at significantly different levels. Here, the expression of *Bbc3* (Puma) and *Pmaip1* (Noxa) is enhanced in the homozygous mutant mice (Fig. 6A). This correlates with an increased occupancy on the corresponding genomic sites by ChIP (Fig. 6D). Such a finding is consistent with the idea that in this tissue, the C terminus somehow interferes with sequence-specific DNA binding and thereby attenuates gene expression. This is selective for *Bbc3* (Puma) and *Pmaip1* (Noxa), as this effect is not seen with *Cdkn1a* (p21) (Fig. 6). In contrast, in the liver, where, again, wild-type and mutant p53 are not expressed at appreciablely different levels, the mRNA levels for *Tigar* are significantly decreased (Fig. 8A), and this is associated with less occupancy on the endogenous *Tigar* gene by the mutant p53 as compared with the FL wild-type protein (Fig. 8D). This latter finding supports a mechanism in which the C terminus is required for sequence-specific DNA binding and subsequent gene activation. Finally, in the liver, *Mdm2* shows reduced gene expression in mutant tissues (Fig. 8A), although gene occupancy is comparable between wild-type and truncated p53 proteins (Fig. 8D). This suggests that the differential regulation is at a step subsequent to DNA binding, most likely because of impaired cofactor recruitment. How does one reconcile such tissue- and target-specific effects? It is possible that existing epigenetic landscapes are established in a p53-independent but tissue-specific manner. This combined with the efficiency of post-translational modifications of the C terminus being different between tissues may thus lead to distinct requirements for target gene expression.

It is intriguing that the overt phenotypic effects of the deletion of the C terminus were restricted primarily to the hematopoietic compartment in homozygous mutant mice. (Figs. 2–4). Since many p53 activities are mediated

through the modulation of the expression of target genes, an attractive hypothesis is that such tissue-specific phenotypes rely on cell type-specific target genes. The expression pattern of *Gfi1* and *Gfi1b*, two essential regulators of hematopoiesis (Hock et al. 2004; van der Meer et al. 2010), is highly restricted to hematopoietic organs (Tong et al. 1998). Both genes are down-regulated in $Trp53^{\Delta CTD/\Delta CTD}$ hematopoietic tissues (Fig. 4D). One of these regulators (Gfi1) was previously shown to be a direct p53 target gene involved in the maintenance of HSC quiescence in a p53-dependent manner (Liu et al. 2009). More recently, Gfi1 was shown to directly interact with p53 and impair its proapoptotic functions in thymocytes, suggesting a possible negative feedback loop (Khandanpour et al. 2013). This would support a model in which Gfi1 interacts with the C terminus of p53, thereby impairing p53 functions. Further characterization of the p53/Gfi1b relationship would be informative. In fact, a rapid survey of the promoter and the first intron of this gene revealed several potential bona fide p53-responsive elements in these regions (data not shown).

Recently, small peptides derived from the p53 C terminus have been proposed as anti-tumorigenic therapeutic agents (Snyder et al. 2004). The data here raise concerns about the use of therapeutic approaches based on small molecules that disrupt the Mdm2–p53 interaction (Vassilev 2007). Increases in p53 protein activity may have unintended consequences on the normal hematopoietic tissues of patients.

In summary, the C-terminal domain of p53 was shown to play key roles in the postnatal homeostasis of the hematopoietic compartment and development of the brain in vivo. Further studies are required to establish the precise molecular pathways at play. Nevertheless, the data indicate that HSCs are highly sensitive to p53 activity and that deletion of the C terminus of p53 can affect key functions and ultimately induce abnormal senescence in mutant bone marrow. Furthermore, the exquisite tissue and target specificity that is observed in these mutant p53 mice have important implications for the role of therapies leading to p53 activation in treatment of tumors of differing origins.

Materials and methods

Generation of the $Trp53^{NEO/NEO}$ and the $Trp53^{\Delta CTD/\Delta CTD}$ mice

The $Trp53^{NEO/NEO}$ mouse was generated by means of a targeting vector harboring two exon 11s separated by a *NEO* selection cassette (see Fig. 1A; Supplemental Material). $Trp53^{NEO/NEO}$ mice were crossed with PrmCre mice (a gift from Dr. Philippe Soriano) (O'Gorman et al. 1997) to generate $Trp53^{NEO/+}$ *CRE*-expressing males. These males were intercrossed with wild-type C57BL/6J females to generate $Trp53^{\Delta CTD/+}$ heterozygous mice. Ultimately, these heterozygous mice were bred to obtain $Trp53^{\Delta CTD/\Delta CTD}$ homozygous animals.

Histopathology and IHC

Mice were placed in 10% formalin for 48 h and then decalcified before sectioning into ~3- to 4-mm coronal sections. Sections were processed and embedded en bloc and stained with haematoxylin and eosin (H&E). One femur from each genotype ($Trp53^{+/+}$, $Trp53^{\Delta CTD/+}$, and $Trp53^{\Delta CTD/\Delta CTD}$) was used to harvest bone marrow for bone marrow brush smears and stained with Diffquik for cytologic evaluation. IHC was performed using the anti-p53 CM5 antibody (Leica Microsystems).

qRT–PCR and immunoblotting

Whole organs were harvested at the indicated times and processed as follows. For RNA preparation, a small sample was excised and submerged in RNAlater RNA stabilization reagent (Qiagen) for later use. The tissue was disrupted and homogenized (PowerGen 125 homogenizer, Fisher Scientific). Total RNA and cDNA were prepared as previously described (Hamard et al. 2012). For protein preparation, a small sample was excised and homogenized into a lysis buffer composed of 50 mM HEPES (pH 7.5), 1% Triton X-100, 150 mM NaCl, 1 mM MgCl2, 1 mM phenylmethylsulfonyl fluoride (PMSF), 5 mg/mL leupeptin, and 50 mg/mL aprotinin. One-hundred micrograms of total protein was resolved by SDS-PAGE. Immunoblot analysis was conducted using the following antibodies: anti-p53 (CM5, Leica Microsystems) and anti-β-actin (Sigma).

Flow cytometry and HSC and fetal liver cell isolation

For determining the percentage of LSK cells, total bone marrow cells were preincubated with 5% rat serum, followed by incubation with c-Kit-FITC, Sca-1-PE, and a biotin-conjugated cocktail containing anti-CD3, anti-CD11b, anti-CD45R/B220, anti-Ly6G, and anti-TER119 (all from BD Biosciences), followed by APC-conjugated streptavidin labeling (eBiosciences). At the end of incubation, the stained cells were treated with DAPI to exclude dead cells and were acquired on either a LSR-II or Fortessa (BD Biosciences). For fetal liver cell staining, pregnant mice were sacrificed at E13.5, fetal liver cells were isolated, and single-cell suspensions were prepared by passing through a cell strainer (70 μM). For fetal liver LSK analysis, anti-CD11b was excluded from the multilineage cocktail. All of the data were analyzed with FlowJo 9.5 software (Tree Star).

Colony-forming unit assay

About 2×10^5 fetal liver cells from E14.5 fetuses of different genotypes were grown on methylcellulose-based medium (MethoCult M3434, Stem Cell Technologies) and maintained in minihumidity chambers in 20% or 5% oxygen tissue culture incubators. After 2 wk, colonies were classified and enumerated based on their morphology. Three types of colonies were counted: colony-forming unit-granulocyte and macrophage (CFU-GM), burst-forming unit-erythroid (BFU-E), and CFU-granulocyte, erythroid, macrophage, and megakaryocyte (CFU-GEMM).

SA-β-Gal assay

Bone marrow cells from P10 whole bone marrow were collected and cytospun on slides. Cells were stained with Senescence-Associated β-Galactosidase Staining kit (Cell Signaling) according to the manufacturer's protocol. Using an inverted microscope and a camera, the number of blue cells were counted and averaged, and a representative picture was taken.

Activated caspase 3 assay

Bone marrow cells from P10 whole bone marrow were collected and cytospun on slides. MEFs derived from E14.5 $Trp53^{+/+}$, $Trp53^{\Delta CTD/+}$, $Trp53^{\Delta CTD/\Delta CTD}$, or $Trp53^{-/-}$ embryos were grown

on coverslips and treated with DOX (Sigma) for 24 h. Both cell types were stained with an anti-cleaved caspase 3 antibody (Cell Signaling, no. 9661S), and immunofluorescence analysis was conducted as previously described (Hamard et al. 2012).

Transplantation experiments

C57/B6 mice were irradiated with a split dose of 6 Gy, 4 h apart. Three hours after the second dose, 0.5×10^6 fetal liver cells from E14.5 *Trp53*$^{+/+}$, *Trp53*$^{\Delta CTD/+}$, *Trp53*$^{\Delta CTD/\Delta CTD}$, or C57/B6 embryos were injected retro-orbitally into ketamine-sedated mice. Mice were monitored for survival on a daily basis. For irradiation control, four mice were irradiated without transplantation for each experiment.

Statistics

Data are represented as means and SEM. Unless otherwise indicated, all experiments were performed in triplicate. A two-tailed student's *t*-test was used for comparison between two groups. $P < 0.05$ was considered significant. One-way ANOVA was used for comparison between more than two groups. $P < 0.05$ was considered significant.

ChIP assay on tissues

Briefly, the organs were dissected from P10 animals, and a single-cell suspension was prepared by crushing them through a 70-μm nylon cell strainer (BD Falcon, catalog no. 352350). Cells were cross-linked in 10 mL of 1% formaldehyde (EM Science, no. FX0415-5) for 10 min at room temperature. The cross-linking reaction was stopped by adding 0.5 mL of 2.5 M glycine to a final concentration of 125 mM for 5 min at room temperature. Cells were spun at 2000 rpm for 5 min, washed once in 1× PBS, and spun again. The remainder of the protocol was previously described (Carvajal et al. 2012) and adapted from Espinosa et al. (2003) using Protein A Dynabeads (Invitrogen) for the pull-down.

Acknowledgments

We thank L. Resnick-Silverman for her help in many aspects of this study. The generation of the embryonic stem cell clones and mouse model was performed in the Transgenic Shared Cored Facility at Mount Sinai. In that regard, K. Kelley is thanked for his expertise in generating the mouse model and his expert advice regarding the maintenance and manipulation of the animals. This work would not have been possible without the enthusiastic advice of P. Soriano and G. Lozano. This work was supported by P01 CA080058 from the National Cancer Institute to J.J.M. and S.A.A. L.A.C. and E.S. were supported by T32 CA078207, also from the National Cancer Institute.

References

Abbas HA, Maccio DR, Coskun S, Jackson JG, Hazen AL, Sills TM, You MJ, Hirschi KK, Lozano G. 2010. Mdm2 is required for survival of hematopoietic stem cells/progenitors via dampening of ROS-induced p53 activity. *Cell Stem Cell* **7:** 606–617.

Ahn J, Prives C. 2001. The C-terminus of p53: The more you learn the less you know. *Nat Struct Biol* **8:** 730–732.

Anderson ME, Woelker B, Reed M, Wang P, Tegtmeyer P. 1997. Reciprocal interference between the sequence-specific core and nonspecific C-terminal DNA binding domains of p53: Implications for regulation. *Mol Cell Biol* **17:** 6255–6264.

Armstrong JF, Kaufman MH, Harrison DJ, Clarke AR. 1995. High-frequency developmental abnormalities in p53-deficient mice. *Curr Biol* **5:** 931–936.

Barlev NA, Liu L, Chehab NH, Mansfield K, Harris KG, Halazonetis TD, Berger SL. 2001. Acetylation of p53 activates transcription through recruitment of coactivators/histone acetyltransferases. *Mol Cell* **8:** 1243–1254.

Basu S, Liu Q, Qiu Y, Dong F. 2009. Gfi-1 represses CDKN2B encoding p15INK4B through interaction with Miz-1. *Proc Natl Acad Sci* **106:** 1433–1438.

Bienz B, Zakut-Houri R, Givol D, Oren M. 1984. Analysis of the gene coding for the murine cellular tumour antigen p53. *EMBO J* **3:** 2179–2183.

Bies J, Sramko M, Fares J, Rosu-Myles M, Zhang S, Koller R, Wolff L. 2010. Myeloid-specific inactivation of p15Ink4b results in monocytosis and predisposition to myeloid leukemia. *Blood* **116:** 979–987.

Bonizzi G, Cicalese A, Insinga A, Pelicci PG. 2012. The emerging role of p53 in stem cells. *Trends Mol Med* **18:** 6–12.

Brosh R, Rotter V. 2009. When mutants gain new powers: News from the mutant p53 field. *Nat Rev Cancer* **9:** 701–713.

Carvajal LA, Manfredi JJ. 2013. Another fork in the road-life or death decisions by the tumour suppressor p53. *EMBO Rep* **14:** 414–421.

Carvajal LA, Hamard P-J, Tonnessen C, Manfredi JJ. 2012. E2F7, a novel target, is up-regulated by p53 and mediates DNA damage-dependent transcriptional repression. *Genes Dev* **26:** 1533–1545.

Ceccaldi R, Parmar K, Mouly E, Delord M, Kim JM, Regairaz M, Pla M, Vasquez N, Zhang Q-S, Pondarre C, et al. 2012. Bone marrow failure in Fanconi anemia is triggered by an exacerbated p53/p21 DNA damage response that impairs hematopoietic stem and progenitor cells. *Cell Stem Cell* **11:** 36–49.

Cellot S, Sauvageau G. 2005. Gfi-1: Another piece in the HSC puzzle. *Trends Immunol* **26:** 68–71.

Chen X, Ko LJ, Jayaraman L, Prives C. 1996. p53 levels, functional domains, and DNA damage determine the extent of the apoptotic response of tumor cells. *Genes Dev* **10:** 2438–2451.

Cheng T, Rodrigues N, Shen H, Yang Y, Dombkowski D, Sykes M, Scadden DT. 2000. Hematopoietic stem cell quiescence maintained by p21$^{cip1/waf1}$. *Science* **287:** 1804–1808.

Cicalese A, Bonizzi G, Pasi CE, Faretta M, Ronzoni S, Giulini B, Brisken C, Minucci S, Di Fiore PP, Pelicci PG. 2009. The tumor suppressor p53 regulates polarity of self-renewing divisions in mammary stem cells. *Cell* **138:** 1083–1095.

Collado M, Serrano M. 2006. The power and the promise of oncogene-induced senescence markers. *Nat Rev Cancer* **6:** 472–476.

Ding L, Morrison SJ. 2013. Haematopoietic stem cells and early lymphoid progenitors occupy distinct bone marrow niches. *Nature* **495:** 231–235.

Donehower LA, Harvey M, Slagle BL, McArthur MJ, Montgomery CAJ, Butel JS, Bradley A. 1992. Mice deficient for p53 are developmentally normal but susceptible to spontaneous tumours. *Nature* **356:** 215–221.

Doulatov S, Notta F, Laurenti E, Dick JE. 2012. Hematopoiesis: A human perspective. *Cell Stem Cell* **10:** 120–136.

Duan Z, Horwitz M. 2005. Gfi-1 takes center stage in hematopoietic stem cells. *Trends Mol Med* **11:** 49–52.

Espinosa JM, Emerson BM. 2001. Transcriptional regulation by p53 through intrinsic DNA/chromatin binding and site-directed cofactor recruitment. *Mol Cell* **8:** 57–69.

Espinosa JM, Verdun RE, Emerson BM. 2003. p53 functions through stress- and promoter-specific recruitment of tran-

scription initiation components before and after DNA damage. *Mol Cell* **12:** 1015–1027.
Feng L, Lin T, Uranishi H, Gu W, Xu Y. 2005. Functional analysis of the roles of posttranslational modifications at the p53 C terminus in regulating p53 stability and activity. *Mol Cell Biol* **25:** 5389–5395.
Greenbaum A, Hsu Y-MS, Day RB, Schuettpelz LG, Christopher MJ, Borgerding JN, Nagasawa T, Link DC. 2013. CXCL12 in early mesenchymal progenitors is required for haematopoietic stem-cell maintenance. *Nature* **495:** 227–230.
Hamard P-J, Lukin DJ, Manfredi JJ. 2012. p53 basic C terminus regulates p53 functions through DNA binding modulation of subset of target genes. *J Biol Chem* **287:** 22397–22407.
He S, Nakada D, Morrison SJ. 2009. Mechanisms of stem cell self-renewal. *Annu Rev Cell Dev Biol* **25:** 377–406.
Hock H, Hamblen MJ, Rooke HM, Schindler JW, Saleque S, Fujiwara Y, Orkin SH. 2004. Gfi-1 restricts proliferation and preserves functional integrity of haematopoietic stem cells. *Nature* **431:** 1002–1007.
Hong H, Takahashi K, Ichisaka T, Aoi T, Kanagawa O, Nakagawa M, Okita K, Yamanaka S. 2009. Suppression of induced pluripotent stem cell generation by the p53-p21 pathway. *Nature* **460:** 1132–1135.
Hu W, Feng Z, Teresky AK, Levine AJ. 2007. p53 regulates maternal reproduction through LIF. *Nature* **450:** 721–724.
Hupp TR, Meek DW, Midgley CA, Lane DP. 1992. Regulation of the specific DNA binding function of p53. *Cell* **71:** 875–886.
Jacks T, Remington L, Williams BO, Schmitt EM, Halachmi S, Bronson RT, Weinberg RA. 1994. Tumor spectrum analysis in p53-mutant mice. *Curr Biol* **4:** 1–7.
Khandanpour C, Phelan JD, Vassen L, Schütte J, Chen R, Horman SR, Gaudreau M-C, Krongold J, Zhu J, Paul WE, et al. 2013. Growth factor independence 1 antagonizes a p53-induced DNA damage response pathway in lymphoblastic leukemia. *Cancer Cell* **23:** 200–214.
Kouzarides T. 2007. Chromatin modifications and their function. *Cell* **128:** 693–705.
Krummel KA, Lee CJ, Toledo F, Wahl GM. 2005. The C-terminal lysines fine-tune p53 stress responses in a mouse model but are not required for stability control or transactivation. *Proc Natl Acad Sci* **102:** 10188–10193.
Kruse JP, Gu W. 2009. Modes of p53 regulation. *Cell* **137:** 609–622.
Kubbutat MH, Jones SN, Vousden KH. 1997. Regulation of p53 stability by Mdm2. *Nature* **387:** 299–303.
Kubbutat MHG, Ludwig RL, Ashcroft M, Vousden KH. 1998. Regulation of Mdm2-directed degradation by the C terminus of p53. *Mol Cell Biol* **18:** 5690–5698.
Liu G, Terzian T, Xiong S, Van Pelt CS, Audiffred A, Box NF, Lozano G. 2007. The p53-Mdm2 network in progenitor cell expansion during mouse postnatal development. *J Pathol* **213:** 360–368.
Liu Y, Elf SE, Miyata Y, Sashida G, Huang G, Di Giandomenico S, Lee JM, Deblasio A, Menendez S, Antipin J, et al. 2009. p53 regulates hematopoietic stem cell quiescence. *Cell Stem Cell* **4:** 37–48.
Luo J, Li M, Tang Y, Laszkowska M, Roeder RG, Gu W. 2004. Acetylation of p53 augments its site-specific DNA binding both in vitro and in vivo. *Proc Natl Acad Sci* **101:** 2259–2264.
Malek R, Matta J, Taylor N, Perry ME, Mendrysa SM. 2011. The p53 inhibitor MDM2 facilitates Sonic Hedgehog-mediated tumorigenesis and influences cerebellar foliation. *PLoS ONE* **6:** e17884.
Manfredi JJ. 2010. The Mdm2-p53 relationship evolves: Mdm2 swings both ways as an oncogene and a tumor suppressor. *Genes Dev* **24:** 1580–1589.
McKinney K, Mattia M, Gottifredi V, Prives C. 2004. p53 linear diffusion along DNA requires its C terminus. *Mol Cell* **16:** 413–424.
Mendrysa SM, Ghassemifar S, Malek R. 2011. p53 in the CNS: Perspectives on development, stem cells, and cancer. *Genes Cancer* **2:** 431–442.
Milyavsky M, Gan OI, Trottier M, Komosa M, Tabach O, Notta F, Lechman E, Hermans KG, Eppert K, Konovalova Z, et al. 2010. A distinctive DNA damage response in human hematopoietic stem cells reveals an apoptosis-independent role for p53 in self-renewal. *Cell Stem Cell* **7:** 186–197.
Molchadsky A, Shats I, Goldfinger N, Pevsner-Fischer M, Olson M, Rinon A, Tzahor E, Lozano G, Zipori D, Sarig R, et al. 2008. p53 plays a role in mesenchymal differentiation programs, in a cell fate dependent manner. *PLoS ONE* **3:** e3707.
Moskovits N, Kalinkovich A, Bar J, Lapidot T, Oren M. 2006. p53 attenuates cancer cell migration and invasion through repression of SDF-1/CXCL12 expression in stromal fibroblasts. *Cancer Res* **66:** 10671–10676.
Mujtaba S, He Y, Zeng L, Yan S, Plotnikova O, Sachchidanand , Sanchez R, Zeleznik-Le NJ, Ronai Z, Zhou MM. 2004. Structural mechanism of the bromodomain of the coactivator CBP in p53 transcriptional activation. *Mol Cell* **13:** 251–263.
O'Gorman S, Dagenais NA, Qian M, Marchuk Y. 1997. Protamine-Cre recombinase transgenes efficiently recombine target sequences in the male germ line of mice, but not in embryonic stem cells. *Proc Natl Acad Sci* **94:** 14602–14607.
Poyurovsky MV, Katz C, Laptenko O, Beckerman R, Lokshin M, Ahn J, Byeon IJ, Gabizon R, Mattia M, Zupnick A, et al. 2010. The C terminus of p53 binds the N-terminal domain of MDM2. *Nat Struct Mol Biol* **17:** 982–989.
Ryan KM, Vousden KH. 1998. Characterization of structural p53 mutants which show selective defects in apoptosis but not cell cycle arrest. *Mol Cell Biol* **18:** 3692–3698.
Sah VP, Attardi LD, Mulligan GJ, Williams BO, Bronson RT, Jacks T. 1995. A subset of p53-deficient embryos exhibit exencephaly. *Nat Genet* **10:** 175–180.
Simeonova I, Jaber S, Draskovic I, Bardot B, Fang M, Bouarich-Bourimi R, Lejour V, Charbonnier L, Soudais C, Bourdon J-C, et al. 2013. Mutant mice lacking the p53 C-terminal domain model telomere syndromes. *Cell Reports* **3:** 2046–2058.
Snyder EL, Meade BR, Saenz CC, Dowdy SF. 2004. Treatment of terminal peritoneal carcinomatosis by a transducible p53-activating peptide. *PLoS Biol* **2:** E36.
Spike BT, Wahl GM. 2011. p53, stem cells, and reprogramming: Tumor suppression beyond guarding the genome. *Genes Cancer* **2:** 404–419.
Suda T, Arai F, Hirao A. 2005. Hematopoietic stem cells and their niche. *Trends Immunol* **26:** 426–433.
Terzian T, Wang Y, Van Pelt CS, Box NF, Travis EL, Lozano G. 2007. Haploinsufficiency of Mdm2 and Mdm4 in tumorigenesis and development. *Mol Cell Biol* **27:** 5479–5485.
Tong B, Grimes HL, Yang TY, Bear SE, Qin Z, Du K, El-Deiry WS, Tsichlis PN. 1998. The Gfi-1B proto-oncoprotein represses p21WAF1 and inhibits myeloid cell differentiation. *Mol Cell Biol* **18:** 2462–2473.
Uccelli A, Moretta L, Pistoia V. 2008. Mesenchymal stem cells in health and disease. *Nat Rev Immunol* **8:** 726–736.
Utikal J, Polo JM, Stadtfeld M, Maherali N, Kulalert W, Walsh RM, Khalil A, Rheinwald JG, Hochedlinger K. 2009. Immortalization eliminates a roadblock during cellular reprogramming into iPS cells. *Nature* **460:** 1145–1148.
van der Meer LT, Jansen JH, van der Reijden BA. 2010. Gfi1 and Gfi1b: Key regulators of hematopoiesis. *Leukemia* **24:** 1834–1843.

Vassilev LT. 2007. MDM2 inhibitors for cancer therapy. *Trends Mol Med* **13:** 23–31.

Vousden KH, Prives C. 2009. Blinded by the light: The growing complexity of p53. *Cell* **137:** 413–431.

Wang YV, Leblanc M, Fox N, Mao JH, Tinkum KL, Krummel K, Engle D, Piwnica-Worms D, Piwnica-Worms H, Balmain A, et al. 2011. Fine-tuning p53 activity through C-terminal modification significantly contributes to HSC homeostasis and mouse radiosensitivity. *Genes Dev* **25:** 1426–1438.

Wolber FM, Leonard E, Michael S, Orschell-Traycoff CM, Yoder MC, Srour EF. 2002. Roles of spleen and liver in development of the murine hematopoietic system. *Exp Hematol* **30:** 1010–1019.

Zheng H, Ying H, Yan H, Kimmelman AC, Hiller DJ, Chen A-J, Perry SR, Tonon G, Chu GC, Ding Z, et al. 2008. p53 and Pten control neural and glioma stem/progenitor cell renewal and differentiation. *Nature* **455:** 1129–1133.